Characterisation of putative retrotrapezoid nucleus (RTN) chemoreceptor neurons in the adult human brainstem

Yazhou Liu[1], Rita Machaalani[2], Irit Markus[1], Claire E. Shepherd*[1,3], Natasha N. Kumar*[1]

[1] Faculty of Medicine and Health, The University of New South Wales, NSW, 2052, Australia

[2] Sydney Medical School, Faculty of Medicine and Health, University of Sydney, NSW, 2006, Australia

[3] Neuroscience Research Australia, Barker Street, NSW, Australia

Corresponding author: Natasha N Kumar (natasha.kumar@unsw.edu.au)

Authors ORCIDS:

Yazhou Liu: 0000-0002-2096-4064

Natasha Kumar: 0000-0003-4712-8792

Rita Machaalani: 0000-0002-7675-1121

Irit Markus: None

Claire Shepherd: 0000-0002-0399-3218

*Co-senior authors

Abstract

The retrotrapezoid nucleus (RTN) of rodents is located ventral to the facial motor nucleus (7N) and consists of acid-sensitive neurons that activate breathing and mediate the central component of the ventilatory response to hypercapnia. In rodents, RTN neurons can be histologically identified by the presence of paired-like homeobox 2B positive nuclei (Phox2b+) and the absence of cytoplasmic choline acetyltransferase (ChAT-) and tyrosine hydroxylase (TH-). Up to 50% of rodent RTN neurons synthesise galanin, and 88% express pituitary adenylate cyclase activating polypeptide (PACAP). The human RTN (hRTN) has not been mapped to date. This study aimed to map the location and cytoarchitecture of the adult hRTN and compare the findings to the homologies of rodents, macaques and human infants. Formalin-fixed, paraffin-embedded tissue blocks from two adult cases, spanning the medulla-pons, were serially sectioned (10µm thick) and every four in thirty sections was assayed for immunohistochemistry for ChAT, or double-labelled Phox2b/TH, Phox2b/galanin and Phox2b/PACAP, followed by analysis using QuPath software. hRTN neurons, identified as Phox2b+/TH-/ChAT-, were located ventral to 7N and lateral to the superior olive, overlapped with the C1 or A5 catecholaminergic population and extended rostrocaudally from Obex +13 to +17 mm. In the parafacial area, 90% of Phox2b immunoreactive (-ir) neurons are hRTN neurons, totaling around 5000 bilaterally, and were surrounded by numerous TH-ir fibers. Galanin- and PACAP-ir was identified in 43% and 39% of Phox2b-ir parafacial neurons, respectively. This is the first study to characterise and quantitatively map the adult human RTN using a series of neurochemical markers.

Keywords

Human RTN, Phox2b, chemoreception, immunohistochemistry, galanin, PACAP

Abbreviations

4V, 4th ventricle; 6N, abducens nucleus; 6n, abducens nerve; 7N, facial motor nucleus; 7n, facial nerve; 8n, vestibulocochlear nerve; A5, A5 catecholaminergic neurons; Biotin-SP-conjugated, biotin-succinimidyl ester conjugated; C1, C1 adrenergic neurons; CCHS, congenital hypoventilation syndrome; ChAT, choline acetyltransferase; CO_2, carbon dioxide; D, dorsal; DAB, 3,3'-

42 diaminobenzidine; DPX, dibutylphthalate polystyrene xylene; FFPE, formalin-fixed, paraffin-
43 embedded; H_2O_2, hydrogen peroxide; H&E, hematoxylin & eosin; hRTN, human retrotrapezoid nucleus;
44 HIER, heat-induced epitope retrieval; icp, inferior cerebellar peduncle; IC, inferior colliculus; IF,
45 immunofluorescence; IgG, immunoglobulin G; IHC, immunohistochemistry; IO, inferior olive; IOP,
46 inferior olive, principal nucleus; -ir, immunoreactivity; IRt, intermediate reticular nucleus; IS, inferior
47 salivatory nucleus; ISH, in situ hybridisation; mcp, medial cerebellar peduncle; ml, medial lemniscus;
48 MSO, medial superior olive; NDS, normal donkey serum; NK1R, neurokinin-1 receptor; NMB,
49 neuromedin B; NTS, nucleus of the solitary tract; PACAP, pituitary adenylate cyclase activating
50 polypeptide; PBS, phosphate-buffered saline; PCRt, parvocellular reticular nucleus; PCRtA,
51 parvocellular reticular nucleus, alpha; Phox2b, paired-like homeobox 2B; PPGAL, preprogalanin; Pn,
52 pontine nuclei; py, pyramidal tract; R, rostral; Rn, Red nucleus; RNA, ribonucleic acid; ROI, regions
53 of interest; RRID, Research Resource Identifier; RTN, retrotrapezoid nucleus; SC, superior colliculus;
54 SLC17A6, solute carrier family 17 member A6 (vesicular glutamate transporter 2 gene); SO, superior
55 olive; Sp5O, spinal trigeminal nucleus, oral part; sp5, spinal trigeminal tract, nerve; TBS, Tris-buffered
56 saline; TH, tyrosine hydroxylase; Thal, thalamus; V, ventral; vGlut2, vesicular glutamate transporter 2;
57 VRC, ventral respiratory column; WB, Western blotting.

58 **Introduction**

59 In mammals, breathing is regulated by central respiratory nuclei and a neural network in the brainstem
60 (Ikeda et al., 2017). Central respiratory chemoreceptors are clusters of cells in the lower brainstem
61 respiratory network which regulate breathing stimulated by carbon dioxide (CO_2) or its proxy, protons
62 (H^+). Acid sensing chemoreceptor neurons in the retrotrapezoid nucleus (RTN) (Guyenet and Bayliss,
63 2015, Guyenet and Bayliss, 2022) project to the ventral respiratory column (VRC) which drives the
64 central respiratory chemoreflex response (Guyenet et al., 2019). Impaired central respiratory
65 chemoreception results in an impaired hypercapnic ventilatory response, as occurs in congenital
66 hypoventilation syndrome (CCHS) and central sleep apnoea (Kasi et al., 2018, Meylemans et al., 2021,
67 Degl'Innocenti et al., 2018, Amiel et al., 2009).

68 The RTN comprises about 2000 neurons in the rat, and 700 - 800 neurons in mice, bilaterally
69 (Takakura et al., 2008, Guyenet and Bayliss, 2015, Shi et al., 2017, Lazarenko et al., 2009). Phox2b is
70 the most widely recognised biomarker for RTN chemoreceptors, and changes in its expression are
71 regarded as an indicator of RTN chemoreceptor dysfunction associated with various central respiratory
72 disorders in both rodents and humans (Amiel et al., 2009, Goridis and Brunet, 2010, Meylemans et al.,
73 2021, Lavezzi et al., 2012). In addition to Phox2b, alterations in neuropeptides, such as galanin and
74 PACAP, are important for regulation of central chemoreception in the RTN. In rodents, galanin is
75 expressed in approximately 50% of RTN neurons (Stornetta et al., 2009) and the PreBotzinger complex
76 receives glutamatergic innervation from galaninergic RTN neurons (Bochorishvili et al., 2012, Dereli
77 et al., 2024). Long term hypercapnia induces an increase in preprogalanin (PPGAL) expression in the
78 RTN (Dereli et al., 2019) and microinjection of galanin into the VRC, specifically in the PreBotzinger
79 and Botzinger complexes, impairs the chemoreflex response to hypercapnia (Abbott et al., 2009). In
80 neonatal mice, PACAP is expressed in 100% of RTN chemoreceptor neurons and the deletion of
81 PACAP in RTN neurons leads to elevated incidence of apnoea's and reduced respiratory responses to
82 CO_2 stimulation in the postnatal period (Shi et al., 2021). Although PACAP expression in the human
83 brainstem has been studied (Huang et al., 2017), the RTN was not investigated due to the lack of
84 knowledge regarding its precise location.

85 To date, four studies have investigated the location of the RTN in primates; 1 in monkeys and
86 3 in humans (Table 1). Levy and colleagues aimed to identify Phox2b mRNA and protein in formalin-
87 fixed, paraffin-embedded (FFPE) adult human brainstem, but it failed to be detected and as such, the
88 data was on a population of PPGAL/ Solute Carrier Family 17 Member A6 (SLC17A6) mRNA
89 containing neurons in the parafacial region (Levy et al., 2021). The other two studies were conducted
90 on FFPE tissue from foetuses or infants (Rudzinski and Kapur, 2010, Lavezzi et al., 2012). Rudzinski
91 and Kapur (2010), described the putative human RTN (hRTN) as a discontinuous cluster of small- to
92 medium-sized Phox2b positive/ Neurokinin 1 receptor positive/Tyrosine hydroxylase negative
93 (Phox2b+/NK1R+/TH-) neurons situated ventral to the facial motor nucleus (7N) and lateral to the
94 superior olivary nucleus (SO) spanning from the caudal pons to the rostral medulla (Rudzinski and

95 Kapur, 2010). Lavezzi et al (2012) described the RTN as a cluster of Phox2b immunoreactive (-ir)
96 neurons situated between the 7N and SO in the caudal pons (Lavezzi et al., 2012). While both infant
97 studies sought to characterise the hRTN, they were restricted by limited tissue sampling and inconsistent
98 Phox2b-ir patterns (Table 1).

99 Since the RTN has not been systematically mapped using Phox2b in the human brainstem, our
100 overall study goal was to fill this research gap. This immunohistochemical study used post-mortem
101 FFPE tissue from 2 adult humans to: 1) characterize Phox2b-ir in the RTN region, 2) establish the
102 neurochemical signature of hRTN neurons and quantify these neurons, 3) establish the neuroanatomical
103 location and dimensions of the hRTN relative to 7N, C1 or A5 catecholaminergic neurons, 4) determine
104 the proportion of parafacial Phox2b-ir neurons expressing the neuropeptides galanin and PACAP, and
105 5) describe the morphological features (size and density) of parafacial Phox2b-ir neurons. Our findings
106 provide valuable insights for investigations into Phox2b-associated disorders, particularly those
107 involving respiratory and autonomic dysfunction including CCHS and sleep apnoea.

108

109 **Table 1:** Summary of data collected on primate RTN in chronological order.

Developmental age, number of cases, Sex ratio	Tissue Frozen or FFPE, and plane of cut (coronal vs sagittal)	Sections/case analysed; Obex/bregma level	Antibody/probe details & dilution	RTN Phox2b subcellular labelling pattern & anatomical location	Number of RTN neurons (bilateral)	Reference
Human fetuses and infants (19-44w, n=8)	5 µm coronal (n=5) and sagittal (n=3) FFPE sections	1-2 sections/case (level not specified but in the presence of the 7N).	Rabbit anti-Phox2b (gift of J.-F. Brunet, 1:1000). NK1R (Abcam, 1:200); TH (Chemicon, 1:1000)	IHC: cell nucleus. RTN was ventral to 7N and lateral to the SO in the pontomedullary junction.	Not provided	(Rudzinski and Kapur, 2010)
Human fetuses (35-40w, n=9) and infant (2-8 months, n=11)	4 µm coronal FFPE sections	3-6 sections/case: 1-2 sections from each brainstem level of upper pons, upper medulla and from Obex -2/3 mm to +2/3 mm.	Rabbit anti-Phox2b (gift of J.-F. Brunet, 1:750)	IHC: cell nucleus and cytoplasm. RTN located between the 7N and SO in caudal pons.	980 ± 23 Phox2b-ir neurons However, equation applied not provided	(Lavezzi et al., 2012)
Macaca fascicularis (5- & 6-years old males and 16-year-old female, n=2 IHC; n=1 ISH)	40 µm coronal frozen and paraformaldehyde fixed free-floating sections	60 sections/case (1/8 serial sections); Obex -1.40mm to +13mm.	IHC: Rabbit anti-Phox2b antibody (1:2,000; gift from J-F. Brunet) ISH: PPGAL and Phox2b mRNAs	IHC: subcellular location of Phox2b immunoreactivity not described. Parafacial region located ventral and lateral to 7N; ISH: cell cytoplasm. PPGAL+/Phox2b+ RTN neurons located caudal, ventral and lateral to 7N spanning from Obex +4.56 to +10.16 mm.	2400 PPGAL+/ Phox2b+ neurons. PPGAL-/Phox2b neurons were not included. Calculated as an estimation by automated method yet cautions on possibility of double counting.	(Levy et al., 2019)
Human adults (n=2)	10 µm coronal FFPE sections	60 sections/case (1/10 serial sections), Obex +14 mm to +17 mm.	mRNA probes (targeting 237–492 sequence of the galanin message-associated peptide mRNA (i.e. PPGAL) and 469–1173 sequence of the vGlut2 mRNA (SLC17A6) and NMB.	IHC: N/A since Phox2b did not work. ISH: N/A since Phox2b did not work. Based on PPGAL, SLC17A6 and NMB, RTN located in parafacial region.	Not provided	(Levy et al., 2021)
Human adults (n=2)	10 µm coronal FFPE sections	90 sections/case (5/30 serial sections), Obex +12 mm to +18 mm.	Mouse anti-Phox2b (Bio-Strategy Laboratory, cat#sc-376997, 1:1000)	IHC: cell nucleus RTN was identified ventral to 7N, lateral to the SO and medial to facial nerve and Sp5O.	Approximately 5000 Phox2b+TH-ChAT- RTN neurons.	Study herein

110

111 **Methods**

112 **Human Tissue Selection**

113 Post-mortem, formalin-fixed brainstem specimens from two adult human cases (76-year-old female,
114 and 87-year-old male; Supplementary Table 1), were sourced from the Sydney Brain Bank through
115 regional brain donor programs in Sydney, Australia. Specimens were acquired from asymptomatic
116 individuals exhibiting solely age-related brain changes and devoid of significant neuropathology.
117 Exclusion criteria included documented respiratory drive disorders, post-mortem delays exceeding 72
118 hours and formalin fixation exceeding ten years. The demographic and autopsy characteristics are
119 presented in Supplementary Table 1.

120 Brainstem tissue blocks spanning from the rostral medulla oblongata (Obex +12 mm) to the
121 caudal pons (Obex +18 mm) were selected (Fig. 1), as this region contains the 7N and is expected to
122 include the hRTN. This Obex range was guided by a human brainstem atlas (Paxinos et al., 2020).

123

124 **Tissue sectioning**

125 Ten-micron serial sections were cut from 2-3 mm thick transverse oriented FFPE brainstem blocks,
126 using a rotary microtome. We collected approximately 700 sections per case, extending rostrocaudally
127 from Obex +18 to +12 mm (Fig. 1). One in every thirty serial sections (300 µm apart) was stained with
128 Hematoxylin & Eosin (H&E), to obtain representative sections containing the 7N. After mapping the
129 full extent of the 7N in H&E sections, four of every thirty serial sections were selected for
130 immunohistochemistry using antibodies against ChAT, Phox2b+TH, Phox2b+PACAP and
131 Phox2b+galanin, respectively (Supplementary Table 2).

132 **Immunohistochemistry (IHC) Protocol for Human FFPE Brain Tissue**

133 The IHC protocol was adapted from our previous methods (Huang et al., 2017), with necessary
134 optimisations for Phox2b detailed in Supplementary Material 1. Antigen retrieval was performed using

135 heat-induced epitope retrieval (HIER) with citrate buffer (pH 6, #S2369, Agilent DAKO) for 15 minutes.
136 After a 2-hour block in 10% normal donkey serum (NDS) in tris buffered saline (TBS) with 0.3% Tween
137 20, sections were incubated overnight with goat anti-ChAT followed by a 2-hour incubation with
138 biotinylated secondary antibody, in 2% NDS /TBS with 0.1% Tween 20 (Table 2). Signal amplification
139 used the Vectastain Elite ABC HRP Kit (#PK-6100, Vector Laboratories), and visualisation was
140 achieved using 3,3'-diaminobenzidine (DAB Substrate Kit, #SK-4100, Vector Laboratories).

141 For dual labelling (Phox2b+TH, Phox2b+PACAP, or Phox2b+galanin), Phox2b was detected
142 first and visualised using DAB with nickel enhancement (black) (#SK-4100, Vector Laboratories). In
143 the sequential round of immunohistochemistry, the tissue was incubated with a primary antibody against
144 TH, PACAP, or galanin, followed by the corresponding secondary antibody and DAB (brown)
145 visualisation. After dehydration and clearing, sections were coverslipped using dibutylphthalate
146 polystyrene xylene (DPX). Antibody details and concentrations are listed in Table 2.

147 **Table 2.** Primary and secondary antibodies used for immunohistochemistry (IHC)

Antibody	Source (Catalogue Number), RRID	Immunogen	Validation	Target & expected subcellular labelling	Dilution
Primary (1°) Antibodies					
Mouse monoclonal anti-Phox2b IgG antibody	Bio-Strategy Laboratory (sc-376997), RRID: AB_2813765	Human origin N-term amino acids 11-70	IHC: cross-reactivity with mouse brain tissue ISH: co-localisation with Phox2b mRNA labelled using RNAscope (Dereli et al., 2021)	Phox2b transcription factor (e.g. nucleus of RTN and C1 neurons)	1:1000
Chicken anti-Tyrosine Hydroxylase (TH)	Aves Labs (TYH-0020), RRID: AB_10013440	Human tyrosine hydroxylase (E.C.1.14.16.2) protein	IF: human gastric tissue (Eicher et al., 2022).	Catecholaminergic neurons (e.g. cytoplasm of C1 neurons)	1:6000
Goat anti-Choline Acetyltransferase (ChAT)	Millipore Sigma (AB144P), RRID: RRID AB_2079751	Human placental enzyme	IHC: rat brain tissue (1:200) (Bhagwandin et al., 2006); IHC: ape brain tissue (1:3000) (Williams et al., 2022)	Cholinergic neurons (e.g. cytoplasm of 7N)	1:1000
Rabbit anti-Galanin	Peninsula Laboratories International (T-4325), RRID: not provided	Synthetic peptide H-Gly-Trp-Thr-Leu-Asn-Ser-Ala-Gly-Tyr-Leu-Leu-GlyPro-His-Ala-Val-Gly-Asn-His-Arg-Ser-Phe-Ser-Asp-Lys-Asn-Gly-LeuThr-Ser-OH coupled to carrier protein.	IHC: human brain tissue (1:300)(Falkenstetter et al., 2020)	Galaninergic neurons (e.g. cytoplasm of NTS and RTN neurons)	1:300
Rabbit anti-PACAP	Abcam (ab216627), RRID: Not provided	Human ADCYAP1 aa 150 to C-terminus	IF: Pig nerve fibers in the aortic arch wall (1:4000) (Rytel et al., 2022); IHC: mouse brain tissue (1:700) (Hu et al., 2020).	PACAP neuropeptide (e.g. cytoplasm of NTS and RTN neurons)	1:300
Secondary (2°) Antibodies					
Biotin-SP-conjugated Donkey anti-Mouse IgG	Jackson ImmunoResearch (715-035-150), RRID: AB_2340770	Whole molecule mouse IgG	WB: Human HeLa cells (1:10000) (Srinivasan et al., 2024)	Mouse anti-Phox2b 1° Ab	1:500
Biotin-SP-conjugated Donkey anti-Chicken IgG	Jackson ImmunoResearch (703-065-155), RRID: AB_2313595	Whole molecule chicken IgY	IHC: mouse eyes (dilution not provided) (Little et al., 2020)	Chicken anti-TH 1° Ab	1:500
Biotin-SP-conjugated Donkey anti-Goat IgG	Jackson ImmunoResearch (705-065-147), RRID: AB_2340397	Whole molecule goat IgY	IHC: Mouse brain and spine tissue (1:500) (Agostinelli et al., 2021)	Goat anti-ChAT 1° Ab	1:500
Biotin-SP-conjugated Donkey anti-Rabbit IgG	Jackson ImmunoResearch (711-065-152), RRID: AB_2340593	Whole molecule rabbit IgY	WB: Human HeLa cells (1:10000) (Srinivasan et al., 2024)	Rabbit anti-PACAP 1° Ab	1:500

148

Microscopy and imaging

Slides were digitised using a slide scanner (Aperio AT2, Leica BioSystems) at 20× magnification. The scanned files were viewed using QuPath Software (Version 0.2.3) (Bankhead et al., 2017). Coronal hemi-sections approximating from Obex +12 to +18 mm were assessed.

The parafacial area was defined as follows: rostrocaudally, spans from the rostral ventrolateral medulla to the caudal ventrolateral pons, located adjacent to the facial motor nucleus (Obex +13 to +17 mm),dorsoventrally and mediolaterally, it is ventral to the spinal trigeminal nucleus, oral part (Sp5O), dorsal to ventral medullary surface, lateral to the intermediate reticular nucleus (IRt) and inferior olive (IO), and medial to the facial nerve (7n) (Fig. 1). Schematic diagrams were drawn using Adobe Illustrator 2024 (Adobe Inc., San Jose, CA, USA).

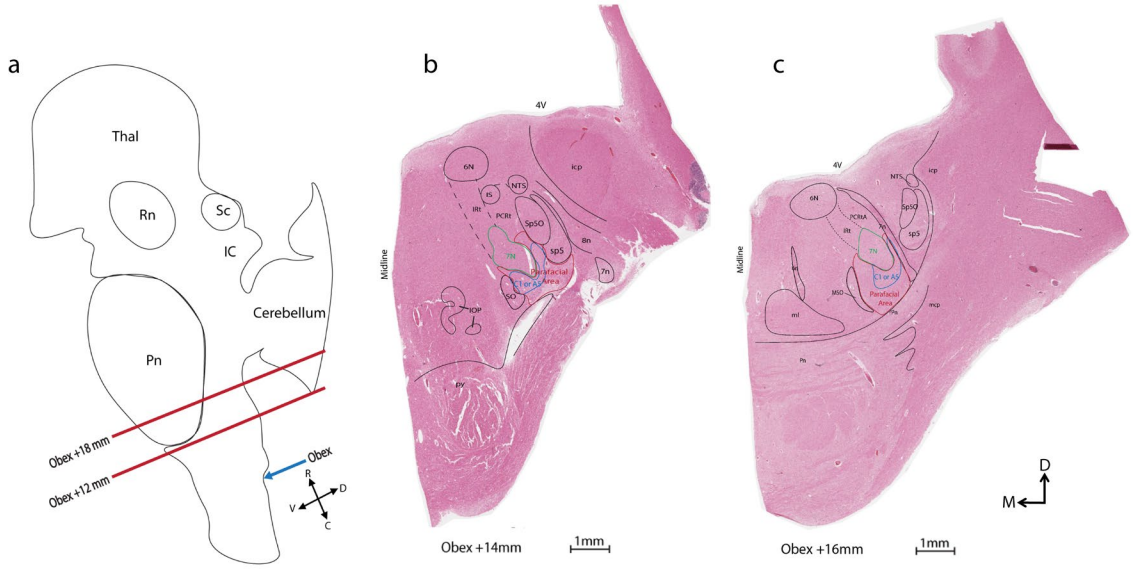

Fig. 1 Tissue sectioning and parafacial area localisation (a) Sagittal schematic of the adult human brainstem and thalamus indicating the angle of tissue sectioning and location spanning from Obex (indicated by blue arrow) +12 to +18 mm (between red lines). (b & c) Representative H&E stained caudal (Obex +14 mm) and rostral (Obex +16 mm) hemi-sections overlaid with brainstem schematics. (b) Caudally, the parafacial (red outline) is encapsulated by a region medial to sp5 and Sp5O, ventral to 7N, lateral to the SO and overlapping with C1 or A5 neurons (blue outline). (c) Rostrally, the parafacial area is medial to 7n, ventral to 7N, lateral to MSO and overlaps with C1 or A5 neurons (blue outline). Adapted from (Paxinos et al., 2020)

Quantitative analyses

169 The cell diameter, and area of the cell soma and nucleus of RTN neurons, were measured using QuPath
170 tools (See details in Supplementary Material 2). This data was collated using Microsoft Excel v14.0
171 (2010, Microsoft, USA), and exported into GraphPad Prism (Version 9, CA, USA).

172 Neurons with the following neurochemical signatures were counted:

173 1- Phox2b immunoreactivity (-ir) parafacial neurons, located ventrolateral to the 7N, as:
174 a. Phox2b-ir RTN neurons: Phox2b+ nucleus, TH- and ChAT- cytoplasm,
175 b. PACAP+/Phox2b+ parafacial neurons and PACAP-/Phox2b+ parafacial neurons,
176 c. Galanin+/Phox2b- parafacial neurons and galanin-/Phox2b+ parafacial neurons,

177 2- 7N neurons as ChAT+ cytoplasm

178 3- C1 neurons: Phox2b+ nucleus, TH+ cytoplasm (Kang et al., 2007, Agostinelli et al., 2023),
179 4- A5 neurons: Phox2b- nucleus, TH+ cytoplasm (Kang et al., 2007, Agostinelli et al., 2023).

180 Phox2b-negative RTN neurons were not investigated in this study. The RTN neurons referred in this
181 study were Phox2b-ir RTN neuron. Number of RTN neurons was calculated by applying the formula
182 derived from (Abercrombie, 1946):

183 Phox2b-ir RTN Cell Count (N) = $RTN\ (Phox2b - ir)\ \ hemisection\ cell\ count\ (n) \times \frac{T}{T+D} \times 2 \times 30$

184 N, Total Phox2b-ir RTN cell count; n, RTN cell count/hemi-section; T, section thickness; D, average
185 diameter of the cell.

186 Morphological data from the 2 adult cases was averaged and presented as mean ± standard deviation.
187 No statistical analysis was performed due to the study being an anatomical description of the hRTN,
188 without comparison between a control and experimental group.

189 **Results**

190 **Immunoreactive labelling profile of antibodies used in this study**

191 The subcellular localisation of labelling for each primary antibody was as expected in positive control
192 regions, including the 7N, NTS and C1 (Fig. 2) (Huang et al., 2017, Kordower et al., 1992, Levy et al.,

193 2019, Agostinelli et al., 2023). ChAT, TH, PACAP and galanin-ir were observed in the cytoplasm and
194 fibers, while Phox2b-ir was confined to the nucleus of neurons (Fig. 2).

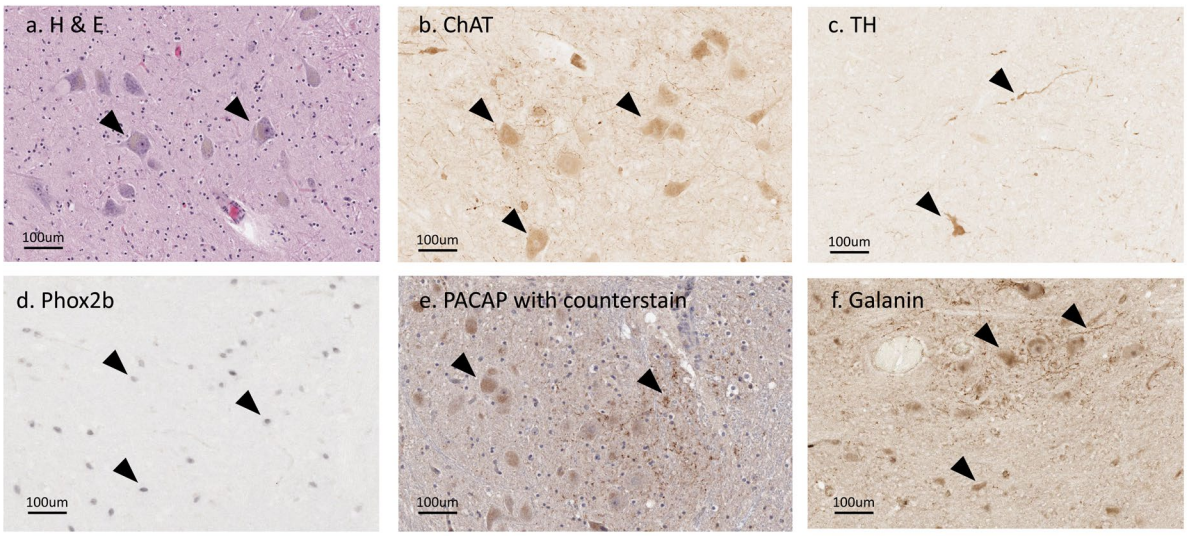

195

196 **Fig. 2 Exemplary H&E and primary antibody labelling.** (a) H&E staining was performed to identify
197 7N neurons, based on their anatomical location. (b) ChAT-ir cytoplasm and fibers in motor neurons
198 within the 7N. (c) TH-ir cytoplasm and fibers in catecholaminergic C1 neurons. (d) Phox2b-ir nuclei in
199 NTS neurons. (e) PACAP-ir cytoplasm and fibers of hematoxylin counterstained NTS neurons. (f)
200 Galanin-ir cytoplasm and fibers in the NTS. Arrowheads point to examples of positive
201 immunoreactivity; arrowheads in (a) and (b) point to the same 7N cells

202 Phox2b-ir was subcategorised as either strong or weak (Supplementary Fig. 1), with cells in each
203 category counted separately before totals were combined (see Supplementary Table 3).

204 **Neurochemical signature of putative hRTN neurons**

205 Identification of RTN neurons according to their biochemical signature of Phox2b+ nucleus, TH-
206 /ChAT- cytoplasm, was clearly discernable from neighboring 7N (ChAT+) and overlapping C1 or A5
207 (TH+) neurons (Fig. 3a, e, f and Supplementary Fig. 2). TH+ fibers coursed through the RTN region
208 (Fig. 3a). In a high magnification image (Fig. 3b), the TH-positive axons were clearly delineated, and
209 TH+ boutons made close appositions with RTN neurons. The subcellular labelling of these
210 neurochemical markers in the RTN and nearby nuclei (7N, C1 or A5) is documented in Table 3. A few
211 Phox2b+/TH- neurons were also detected in Sp5O (Fig. 3c), IRt and parvocellular reticular nucleus
212 (PCRt) (Fig. 3d).

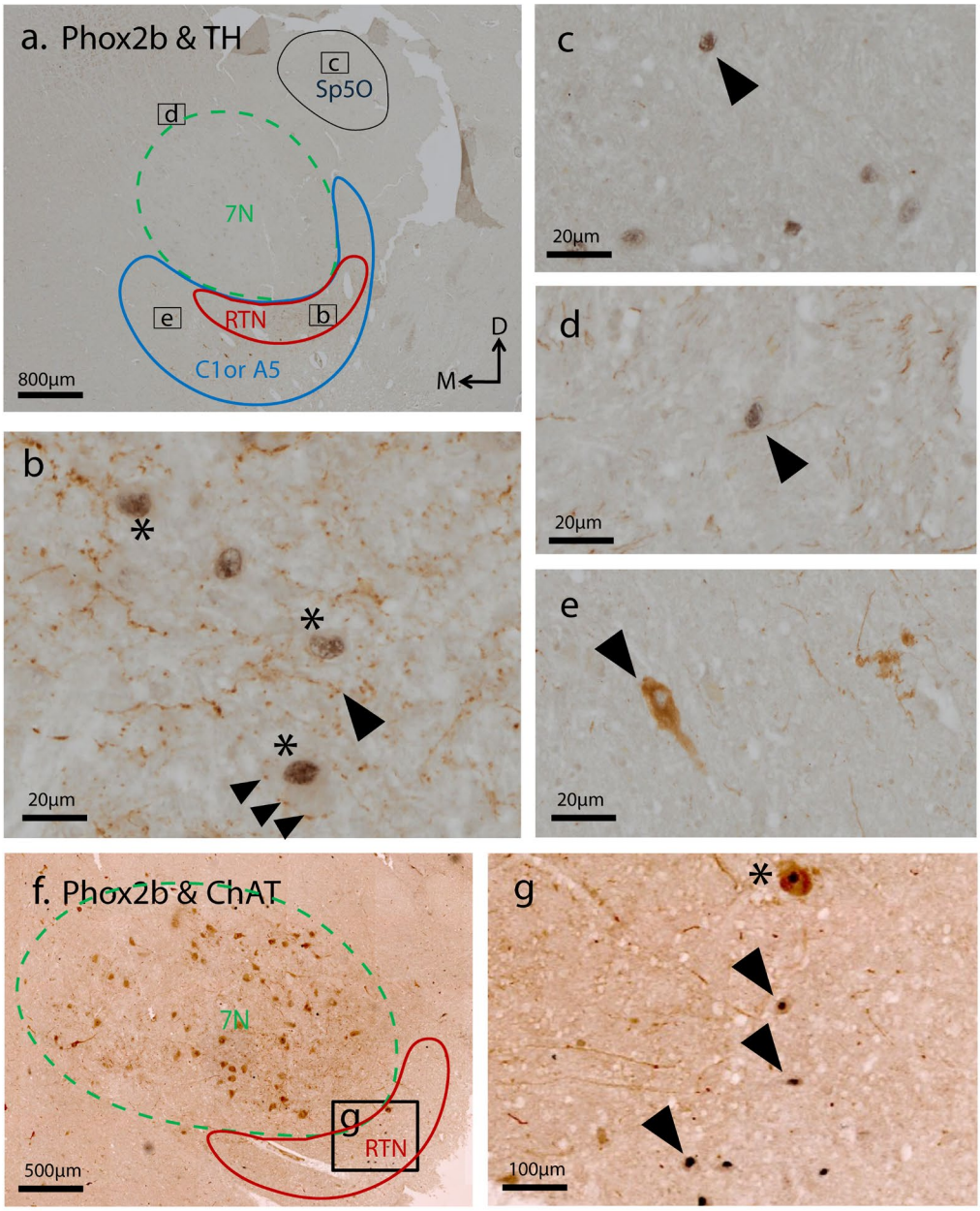

Fig. 3 RTN neurochemical signature and spatial relationship to 7N, C1 or A5. (a) Low-magnification image showing the anatomical locations of the RTN (red outline), C1 or A5 region (blue outline), Sp5O (black outline), and 7N (green outline) within the brainstem. (b) Dual immunohistochemistry for Phox2b and TH identified RTN neurons as Phox2b+ with nuclear localisation (asterisks), and TH- cytoplasm, distinguishing RTN neurons from C1 or A5 neurons. Numerous TH-ir fibers (arrowheads) were present in the RTN region and closely apposed Phox2b-ir neurons (asterisks). (c) Sp5O neurons exhibited Phox2b-ir (arrowhead). (d) A few sparsely distributed Phox2b+/TH- neurons were detected in the IRt, dorsomedial to the 7N (arrowhead). (e) A5 neuron expressing TH-ir in the cytoplasm. (f) Low power image illustrating the location of the RTN (red outline) ventral to the 7N (green outline) in the brainstem (Obex +15 mm). (g) Phox2b and ChAT double

224 immunohistochemical detection demonstrate RTN neurons as Phox2b+ and ChAT- (arrowheads). In
225 contrast, the 7N neurons (asterisk) were identified by their ChAT+ soma and relatively large diameter

226 **Phox2b+ parafacial neurons are immunoreactive for galanin and PACAP**

227 Although TH immunohistochemistry was not performed in combination with Phox2b/PACAP or
228 Phox2b/galanin labelling, our quantitative data show that 90% of Phox2b-ir neurons located ventral to
229 7N are devoid of TH-ir (Fig. 3b). This strongly suggests that these neurons are part of the RTN
230 population. Therefore, in this context, we confidently identified RTN neurons based on their Phox2b
231 expression and anatomical location within the parafacial region. Based on the double labelling for
232 Phox2b and galanin as well as the double labelling for Phox2b and PACAP, a total of 5295 Phox2b+
233 parafacial neurons were counted (Table 4).

234 Galanin-ir was detected in the soma and dendrites of Phox2b-ir parafacial neurons (Fig. 4a-c)
235 and represented 43% of total Phox2b-ir population (2262 galanin+/Phox2b+ neurons out of 5295
236 Phox2b+ parafacial neurons) (n=2, with 14 sections counted per case) (Supplementary Table 3).
237 Similarly, PACAP-ir was confined to cell soma and dendrites of 39% Phox2b-ir parafacial neurons
238 (2090 PACAP+/Phox2b+ parafacial neurons out of 5295 Phox2b-ir parafacial neurons, Fig. 4d-f,
239 Supplementary Table 3).

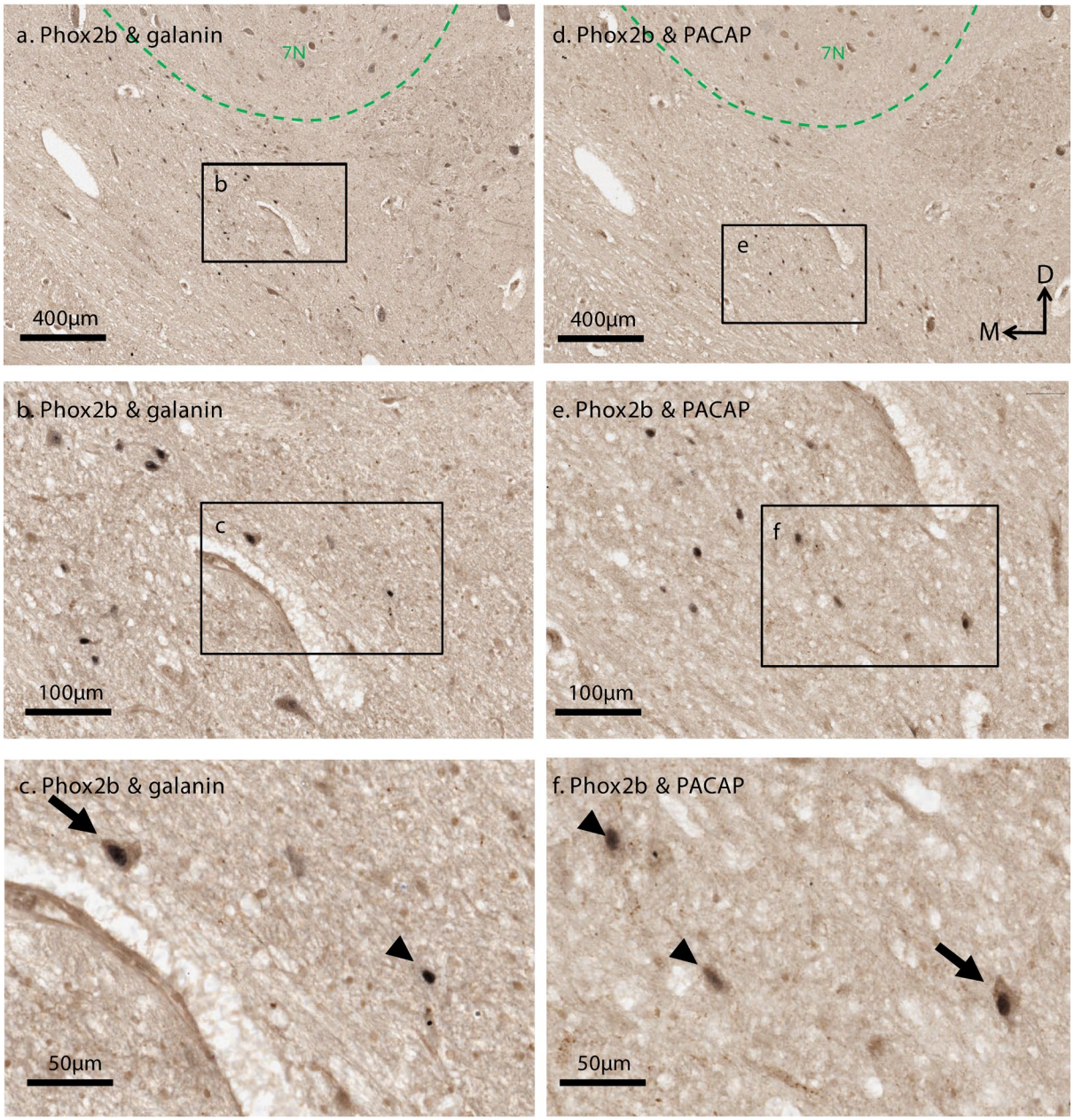

Fig. 4 Galanin and PACAP immunoreactivities are detectable in large subsets of Phox2b-ir parafacial neurons. (a and d) Low magnification image of the RTN region immediately ventral to the 7N. (b) Many neurons in the parafacial region are both galaninergic (brown cytoplasmic labelling) and Phox2b-ir (black nucleus labelling). (c) Magnification of inset in b) demonstrating a galanin+/Phox2b+ neuron (arrow) and a galanin-/Phox2b+ neuron (arrowhead). (e) A subgroup of neurons in the parafacial region display PACAP-ir (brown cytoplasmic labelling) and Phox2b-ir (black nucleus labelling). (f) Magnification of inset in (e) demonstrating PACAP+/Phox2b+ neuron (arrow) and PACAP-/Phox2b+ neurons (arrowheads)

Anatomical characteristics of the hRTN based on the distribution of Phox2b+/TH- neurons

250 Putative hRTN neurons were located ventral and ventrolateral to the 7N, lateral to the SO, dorsomedial
251 to the pontomedullary junction, medial to the Sp5O, spinal trigeminal tract (sp5) and the facial nerve,
252 and overlapping with C1 or A5 catecholaminergic neurons (Fig. 3).

253 RTN neurons were found from Obex +13 to +17 mm (Fig. 5 and Fig. 6) of the medulla
254 oblongata. At caudal levels, Obex +13 to +13.8 mm, RTN neurons were sparsely distributed (Fig. 5 and
255 Fig. 6a). By contrast, within the range of +13.8 to +14.8 mm, RTN neurons formed a distinct and
256 prominent cluster (Fig. 5), indicated by a concentrated presence of Phox2b+/TH- neurons. More
257 rostrally, (+14.8 to +16.8 mm), the RTN neurons were again more sparsely distributed, devoid of a
258 distinct cluster (Fig. 5 and Fig. 6c). Anatomically, rostral RTN neurons were distributed medial to the
259 facial nerve, ventrolateral to the 7N, dorsal to the ventral surface of medulla and lateral to the SO (Fig.
260 5).

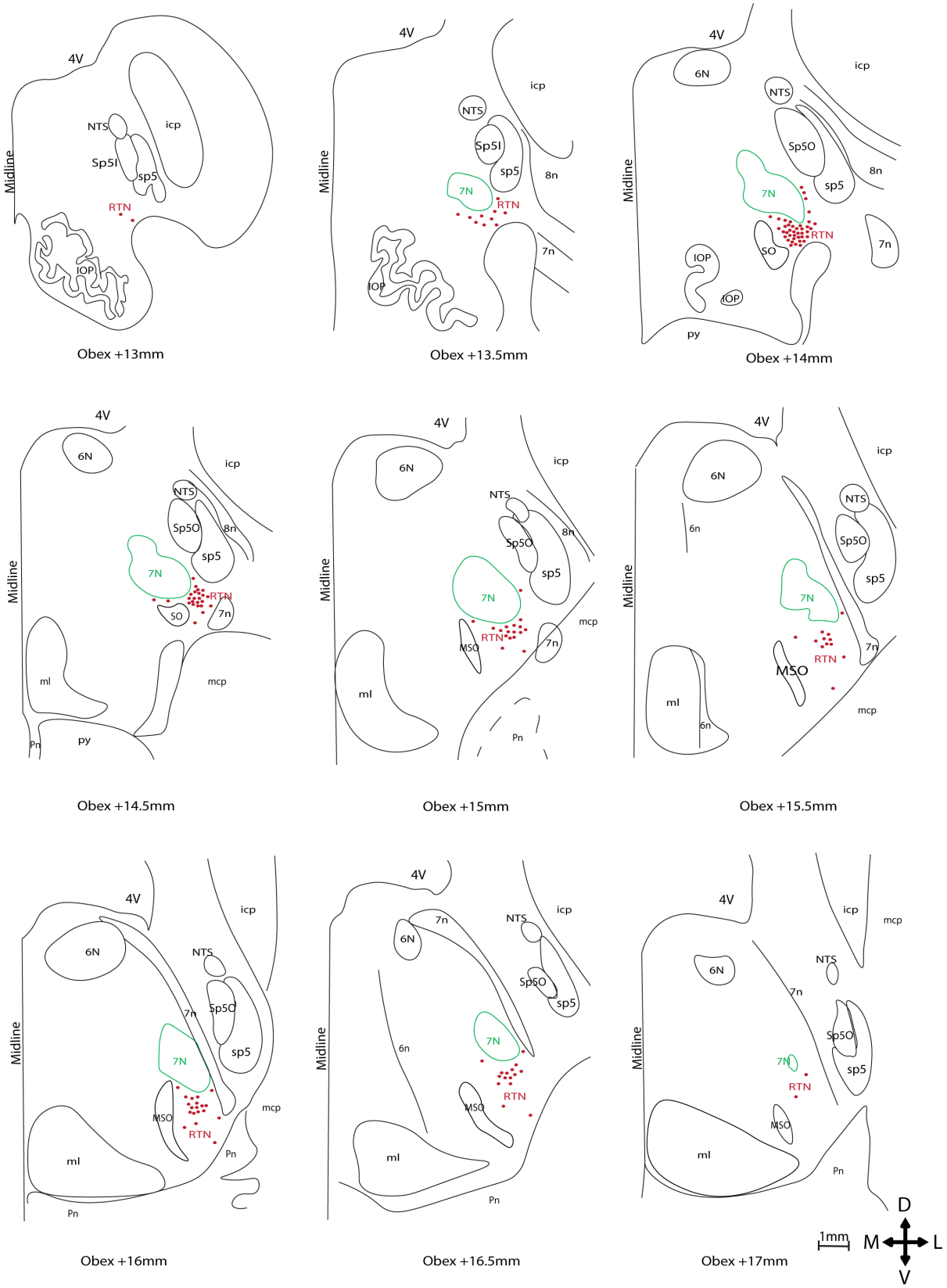

261

262 **Fig. 5 Schematic coronal hemi-sections illustrating the distribution of parafacial Phox2b+/TH-**
263 **neurons, representative of the RTN (from Obex +13 to +17 mm).** Red dots represent
264 Phox2b+/TH- neurons. RTN neurons are located immediately ventral to the 7N, lateral to the SO, and
265 medial to the facial nerve (rostrally) or spinal trigeminal nucleus (caudally). The most densely packed

cluster of RTN neurons is situated 14 mm rostral to Obex. Drawings were made with reference to (Paxinos et al., 2020)

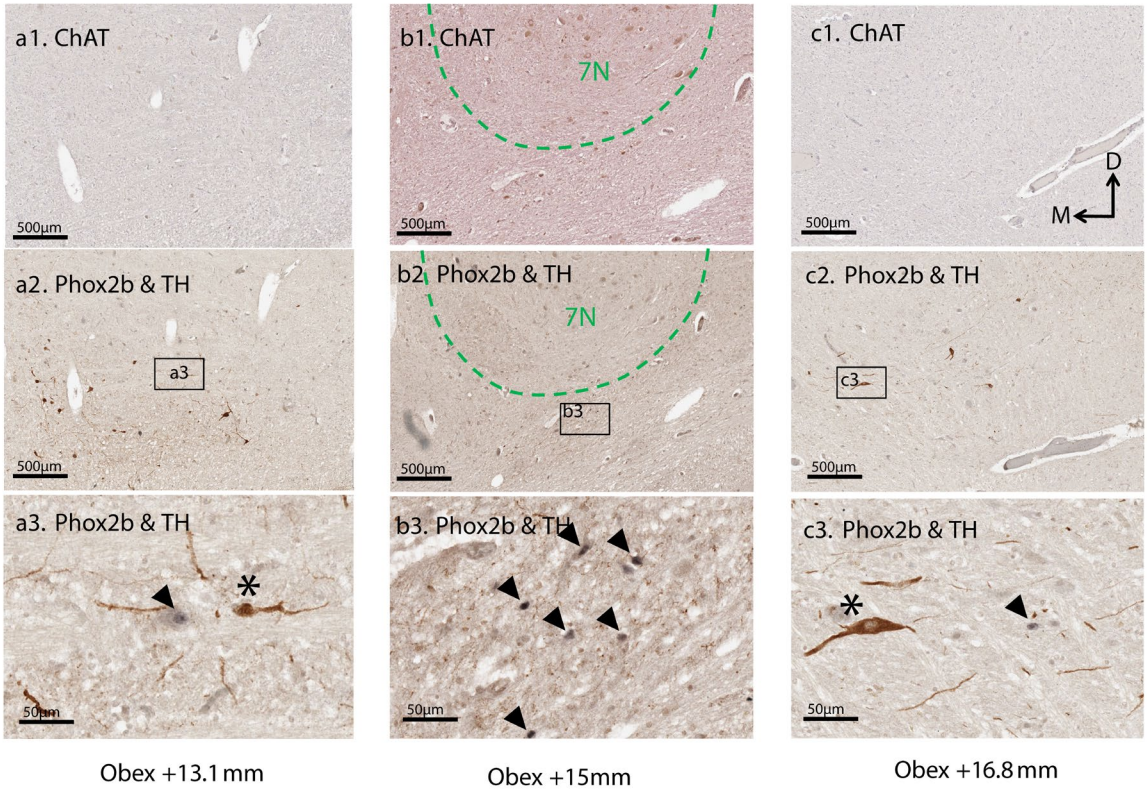

Fig. 6 RTN neurons extend along the entire rostrocaudal length of the 7N. (a1 and a2) Caudal pole of the 7N (Obex +13.1 mm). (a3) C1 neuron (TH-ir, asterisk) next to an RTN neuron (arrowhead). (b1 and b2) 7N neurons are distinguished from the RTN region by the green outline. (b3) RTN neurons (Phox2b+/TH-, arrowheads) and TH-ir fibers (brown puncta) are notably abundant at this level of the RTN. (c1 and c2) Rostral pole of the 7N (Obex +16.8 mm). (c3) Few RTN neurons (Phox2b+/TH-, arrowhead) were present. An A5 neuron (Phox2b-/TH+, asterisk) is visible in the rostral RTN region

Morphology of hRTN neurons

The soma of RTN neurons was typically round, or fusiform, with one or two dendrites extending in various directions (Fig. 4). RTN neurons were significantly smaller in size compared to 7N, C1 or A5 neurons, with an average soma area of 309.9 ± 61.8 µm² (n=241 cells), and an average nucleus area of 69.0 ± 23.3 µm² (Table 3).

281 **Table 3. Morphological characteristics of RTN, 7N, C1 and A5 neurons, based on their**
282 **respective subcellular neurochemical signature**

Cell Type	Morphology	Nucleus: Area (μm^2)	Cell Area (μm^2)	Cell Diameter (μm)	Subcellular neurochemical profile		
					Cytoplasm	Nucleus	Axon
7N neurons (n=68, 1 section/case)	Large multipolar neurons with short dendrites	274.6 ± 108	1194.0 ± 371.8	41.8 ± 10.7	ChAT+, TH-, PACAP+/-, galanin-	Phox2b+/-	ChAT+
RTN neurons (n=241, 3 sections/case)	Medium round or fusiform neurons with short dendrites	69.0 ± 23.3	309.9 ± 61.8	19.9 ± 4.0	ChAT-, TH-, PACAP+/-, Galanin+/-	Phox2b+	Not detected
C1 neurons (n=38, 4 sections/case)	Medium multipolar neuron with short dendrites and long projecting axons	98.0 ± 51.2	528.2 ± 165.2	35.1 ± 8.9	ChAT-, TH+, PACAP+/-, galanin-	Phox2b+	TH+
A5 neurons (n=12, 4 sections/case)	Medium multipolar neuron with short dendrites and long projecting axons	101.3 ± 44.9	468.7 ± 169.4	33.9 ± 11.7	ChAT-, TH+, PACAP+/-, galanin-	Phox2b-	TH+

Mean ± standard deviation.

283

284 **Quantification of hRTN neurons**

285 Based on Phox2b+/TH- immunoreactivity, the number of putative RTN neurons ranged from 5 to 65
286 per hemi-section, with a peak observed between Obex +14.0 mm and +14.3 mm (Fig. 7a). Considering
287 both weak and strong Phox2b-ir, the total number of RTN neurons was 5300 and 4903 (n=2 cases,
288 Table 4), spanning 4 mm in rostrocaudal length (Fig. 7a) and ~1.5-2 mm in dorsoventral length (Fig. 5)

289 The rostrocaudal distribution of galanin+/Phox2b+ and PACAP+/Phox2b+ parafacial neurons
290 followed the same trend, showing a peak in counts at Obex 14 mm and spanning 4 mm in rostrocaudal
291 length (Fig. 7b and 7c). From these double labelled sections, a total of 5295 Phox2b-ir parafacial
292 neurons were counted (Table 4). The galanin population was 43% of the total Phox2b-ir population
293 while PACAP was 39% (Table 4).

294

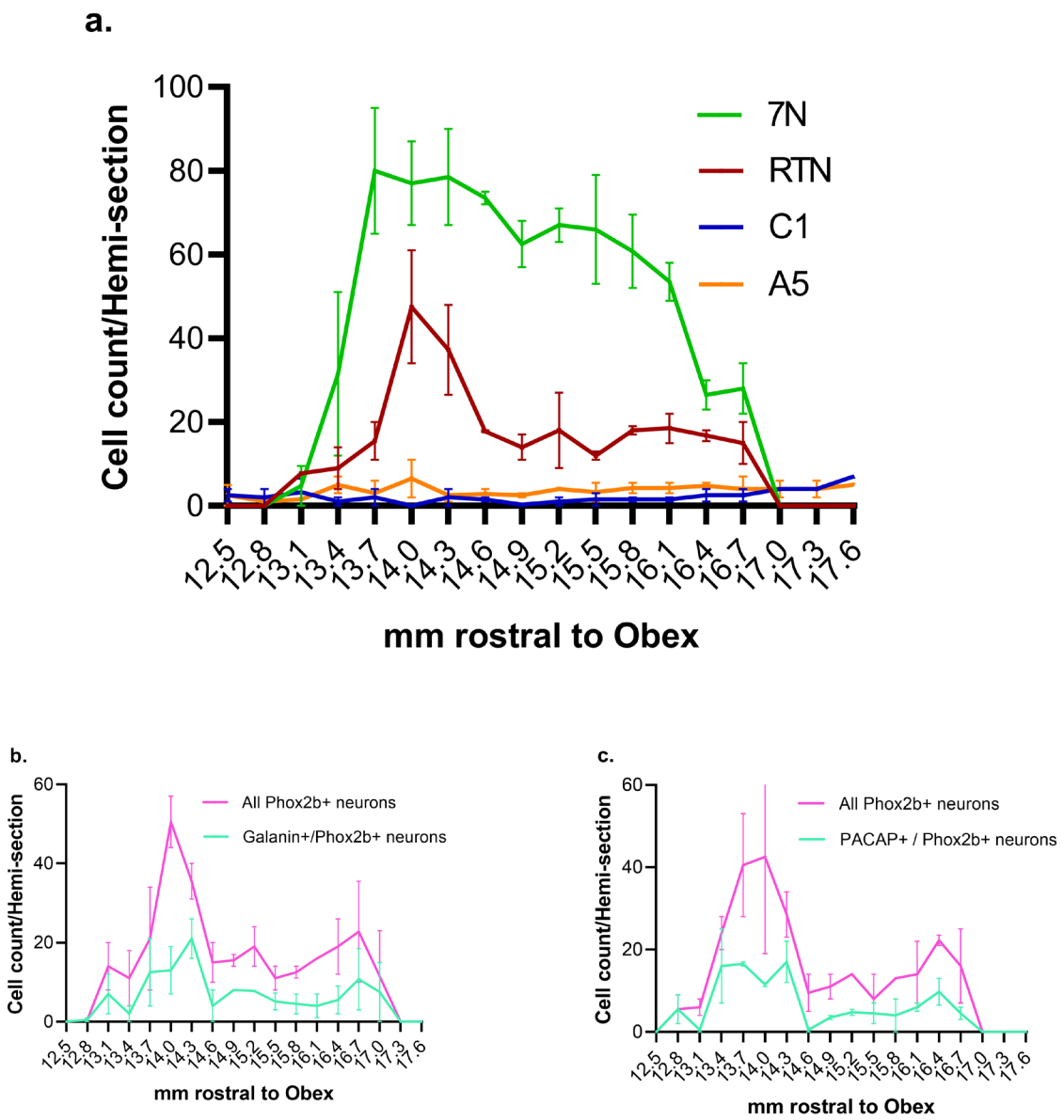

295

296 **Fig. 7 Cell count of the RTN, 7N, C1 and A5 neurons.** (a) Rostral-caudal distribution and
297 quantification RTN (Phox2b+/TH-), C1 (Phox2b+/TH+) and A5 (Phox2b-/TH+) neurons within the
298 region of interest specified in Fig. 1b and Fig. 1c. Additionally, total 7N (ChAT+) neurons were
299 counted. The rostral-caudal distribution of (b) Galanin+/Phox2b+ neurons and (c) PACAP+/Phox2b+
300 neurons, in the RTN region. The curves represent the average number of cells/hemi-section (n=2).
301 The vertical bars indicate interindividual variability in RTN, 7N, C1, and A5 neuron counts observed
302 between the two human cases.

303

304 **Table 4.** Total Phox2b-ir parafacial neurons and the proportion that are galanin-ir or PACAP-ir*

	Phox2b+ RTN neurons *	Phox2b+ parafacial neurons	Phox2b+/ PACAP+ parafacial neurons	Phox2b+/galanin+ parafacial neurons	% of Phox2b+ parafacial PACAP+ neurons	% of Phox2b+ parafacial galanin+ neurons
Case 1	5300	5960	2420	2985	41	50
Case 2	4903	4630	1760	1540	38	33
Average	5102	5295	2090	2262	39	43

*Refer to Supplement Table 3 for the breakdown of the counts according to labelling intensity.

305

306 **Discussion**

307 This study provides a comprehensive characterisation of the adult human RTN using histological and
308 neuroanatomical means. Leveraging previous reports from infant, macaque and rodent studies, we
309 identified a large cluster of Phox2b+/TH- neurons ventral to the 7N, aligning with the expected location
310 of the RTN. We present the first in-depth analysis of Phox2b+ RTN neurons, detailing their rostrocaudal
311 distribution, cell counts, morphology and expression of respiratory-related neuropeptides - galanin and
312 PACAP. We also demonstrate puncta from TH+ fibers in close apposition to RTN neurons. These
313 findings establish a crucial baseline for assessing age-related or disease-related changes in the RTN,
314 such as neuronal loss, or altered neuropeptide expression, in respiratory and neurological disorders.

315 **Adult human RTN neurons are Phox2b positive and subsets express galanin and PACAP**
316 **immunoreactivity**

317 In this study, the adult hRTN was identified using histological criteria established for identification of
318 RTN neurons in rodents; namely, parafacial neurons that express the transcription factor Phox2b and
319 are devoid of TH and ChAT immunoreactivity (Guyenet and Bayliss, 2022). We identified a highly
320 circumscribed cluster of Phox2b neurons in adult hRTN, in agreement with findings in infants.
321 Approximately 43% of these neurons co-expressed galanin, closely aligning with findings from adult
322 rats (Stornetta et al., 2009). Furthermore, the number of galanin-ir neurons we identified (2,262) is
323 comparable to the ~2,400 reported in the macaque RTN (Levy et al., 2019). Our study is the first to
324 demonstrate PACAP expression in hRTN, with 40% of Phox2b-ir parafacial neurons co-expressing
325 PACAP. This proportion is substantially lower than what has been reported in adult mice, where

326 PACAP is expressed in 100% of RTN chemoreceptors in neonates and 88% in adulthood (Shi et al.,
327 2017, Shi et al., 2021).

328 **The location of hRTN neurons in the adult is highly consistent with the distribution reported in**
329 **human infants and other species**

330 In this study, the spatial distribution of adult hRTN neurons closely aligns with findings from rodents,
331 non-human primates, and human infants (Levy et al., 2019, Levy et al., 2021, Lavezzi et al., 2012,
332 Rudzinski and Kapur, 2010, Shi et al., 2017). Dorsoventrally, the hRTN neurons are situated dorsal to
333 the pontomedullary junction, lateral to the superior olive, and ventrolateral to the 7N. Rostrocaudally,
334 hRTN neurons extended from Obex +13 to +17 mm. A previous study in adults reported
335 PPGAL+/VGlut2+ putative hRTN neurons extending from Obex +14 to +17 mm (Levy et al., 2021).
336 This shorter rostrocaudal extent observed is potentially due to discrepancies between versions of human
337 brainstem atlases. Notably, the Paxinos 2012 atlas used by Levy et al, describes the facial motor nucleus
338 as 3 mm long, while the updated 2020 version used in our study reports it as 4 mm in rostrocaudal
339 length. Nevertheless, both studies demonstrate close proximity between the RTN and 7N throughout
340 their rostrocaudal extent, underscoring the reliability of the findings.

341 Another key difference between our study and Levy's (Levy et al., 2021) is the biomarkers used
342 to identify RTN neurons. While our study successfully detected Phox2b-ir, Levy et al. relied on vGlut2
343 and PPGAL co-expression, however, they did not define the non-galaninergic RTN neurons (Levy et
344 al., 2021) leading to an underestimation of RTN neurons. Thus, our dataset represents the most complete
345 count of RTN neurons to date including both galanin+ and galanin- RTN neurons.

346 **The adult human contains more RTN neurons than adult rodents and macaque**

347 We identified approximately 5000 Phox2b+/TH- neurons within the putative hRTN, bilaterally, a count
348 significantly higher than the approximately 980 Phox2b-ir neurons reported in human infants (Lavezzi
349 et al., 2012). The discrepancy may stem from differences in immunohistochemistry protocol, or the
350 exclusion of "weakly" Phox2b-ir neurons from the RTN population in earlier studies (Lavezzi et al.,
351 2012, Levy et al., 2019). However, even when counting only strongly Phox2b-ir neurons, we found an

352 average of 2530 per case bilaterally, which is still significantly greater than the 980 reported by Lavezzi
353 et al. (Lavezzi et al., 2012). Since RTN neuron numbers remain stable from late prenatal stages to
354 adulthood in rodents, developmental stage is unlikely the cause. Direct comparisons across studies
355 would require consistent tissue preservation, antigen retrieval and immunohistochemical protocols.
356 Species comparisons report bilateral RTN counts of ~2,000 in rats (Stornetta et al., 2009, Takakura et
357 al., 2008), ~700 in mice (Lazarenko et al., 2009, Shi et al., 2017), and ~2,400 galaninergic neurons in
358 macaques (Levy et al., 2019). Our higher count in humans likely reflects both true interspecies
359 differences and methodological factors such as more extensive serial sectioning and variations in RTN
360 rostrocaudal length across atlases (Paxinos, 2012, Paxinos et al., 2020). Some earlier studies did not
361 assess serial sections and based total cell counts on only 1-2 sections per case (Lavezzi et al., 2012,
362 Rudzinski and Kapur, 2010). Notably, our female case had 29% more RTN neurons than the male,
363 suggesting possible sex or inter-individual differences that warrant further investigation.

364 **C1-RTN circuit and its role in breathing control: evidence of neuronal interactions**

365 In this study, we show that TH-ir presumptive C1 neurons are intermingled with RTN neurons, and our
366 data suggest close appositions between TH-ir terminals and RTN neurons. Rodent studies have
367 demonstrated that the RTN is dense with PNMT-ir terminals (Rosin et al., 2006) and vigorously
368 activated by adrenaline via α1 adrenoceptors (Oliveira et al., 2016). Furthermore, optogenetic
369 stimulation of C1 neurons in rats produces respiratory effects similar to RTN photo-stimulation (Souza
370 et al., 2020), suggesting a functional C1-RTN circuit in the central control of breathing. These findings
371 suggest that hRTN neurons receive projections from C1 catecholaminergic neurons, however, further
372 studies are needed to confirm the origin of the TH-ir axons and boutons apposing hRTN neurons.

373 **Factors affecting RTN neuronal counts and future research directions**

374 The RTN neuronal cell count may be influenced by several factors. First, the neurochemical signature
375 used to define RTN neurons could inadvertently include Phox2b+/TH- PCRt, IRt or Sp5O neurons
376 located in the region dorsal and medial to 7N (Fig. 3d), However these were excluded from hRTN
377 because their distribution was anatomically discontinuous from the RTN cluster. Secondly, although

this study identified hRTN neurons based on the neurochemical signature established in rodent functional studies (Lazarenko et al., 2009), further research is needed to confirm that these Phox2b+/TH- neurons are indeed chemosensory (Shi et al., 2017). Third, we have reported RTN neuron counts in older adults, and it is uncertain whether Phox2b-ir neurons undergo age-related degeneration. If such degeneration occurs, our quantitative results may underestimate the number of Phox2b-ir RTN neurons in young adults. Finally, although this study was limited by a small sample size, a key strength lies in our thorough analysis of the entire length of the RTN (14 sections per case, spanning 4mm rostrocaudally), rather than focussing on a single plane as is common in studies using post-mortem human brain tissue. A further strength is the consistent rostral-caudal distribution and the quantified peaks of RTN neurons observed across the two cases. Future studies with a larger sample size are needed to evaluate changes in this neuronal population with age, sex and disease, strengthening the robustness and generalisability of our findings. Our study lays the groundwork for these future investigations and for future studies investigating changes in disorders affecting central respiratory chemoreception.

Conclusion

This study mapped the full extent of the adult hRTN using established neurochemical and anatomical markers, locating it ventral to 7N, lateral to the superior olive, and overlapped with C1 or A5 catecholaminergic neurons. Extending rostrocaudally from Obex +13 to +17 mm, the hRTN contains around 5000 neurons bilaterally - comprising 90% of Phox2b-ir neurons in the parafacial area - surrounded by dense TH-ir fibers. Approximately 40% of these neurons express galanin and PACAP. The data herein provides baseline values for future studies in clinical contexts such as CCHS and sleep apnoea.

Acknowledgements

This work was supported by grants from Australian Research Council (grant no. DP180101890). Tissues were received from the Sydney Brain Bank which is supported by Neuroscience Research

Australia and a special gift in memory of Jim Raftos from the Shaw family. We thank Prof Patrice G Guyenet and Prof Ruth Stornetta for providing feedback on an advanced version of the manuscript.

References

ABBOTT, S. B., BURKE, P. G. & PILOWSKY, P. M. 2009. Galanin microinjection into the PreBotzinger or the Botzinger Complex terminates central inspiratory activity and reduces responses to hypoxia and hypercapnia in rat. *Respir Physiol Neurobiol,* 167**,** 299-306.http://dx.doi.org/10.1016/j.resp.2009.06.003

ABERCROMBIE, M. 1946. Estimation of nuclear population from microtome sections. *The Anatomical Record,* 94**,** 239-247.http://dx.doi.org/https://doi.org/10.1002/ar.1090940210

AGOSTINELLI, L. J., SEAMAN, S. C., SAPER, C. B., et al. 2023. Human Brainstem and Cerebellum Atlas: Chemoarchitecture and Cytoarchitecture Paired to MRI. *J Neurosci,* 43**,** 221-239.http://dx.doi.org/10.1523/JNEUROSCI.0587-22.2022

AMIEL, J., DUBREUIL, V., RAMANANTSOA, N., et al. 2009. PHOX2B in respiratory control: lessons from congenital central hypoventilation syndrome and its mouse models. *Respir Physiol Neurobiol,* 168**,** 125-32.http://dx.doi.org/10.1016/j.resp.2009.03.005

BANKHEAD, P., LOUGHREY, M. B., FERNANDEZ, J. A., et al. 2017. QuPath: Open source software for digital pathology image analysis. *Sci Rep,* 7**,** 16878.http://dx.doi.org/10.1038/s41598-017-17204-5

BOCHORISHVILI, G., STORNETTA, R. L., COATES, M. B., et al. 2012. Pre-Bötzinger complex receives glutamatergic innervation from galaninergic and other retrotrapezoid nucleus neurons. *J Comp Neurol,* 520**,** 1047-61.http://dx.doi.org/10.1002/cne.22769

DEGL'INNOCENTI, D., BECATTI, M., PERUZZI, M., et al. 2018. Systemic oxidative stress in congenital central hypoventilation syndrome. *Eur Respir J,* 52.http://dx.doi.org/10.1183/13993003.01497-2018

DERELI, A. S., OH, A. Y. S., MCMULLAN, S., et al. 2024. Galaninergic and hypercapnia-activated neuronal projections to the ventral respiratory column. *Brain Struct Funct,* 229**,** 1121-1142.http://dx.doi.org/10.1007/s00429-024-02782-8

DERELI, A. S., YASEEN, Z., CARRIVE, P., et al. 2019. Adaptation of Respiratory-Related Brain Regions to Long-Term Hypercapnia: Focus on Neuropeptides in the RTN. *Front Neurosci,* 13**,** 1343.http://dx.doi.org/10.3389/fnins.2019.01343

GORIDIS, C. & BRUNET, J. F. 2010. Central chemoreception: lessons from mouse and human genetics. *Respir Physiol Neurobiol,* 173**,** 312-21.http://dx.doi.org/10.1016/j.resp.2010.03.014

GUYENET, P. G. & BAYLISS, D. A. 2015. Neural Control of Breathing and CO2 Homeostasis. *Neuron,* 87**,** 946-61.http://dx.doi.org/10.1016/j.neuron.2015.08.001

GUYENET, P. G. & BAYLISS, D. A. 2022. Central respiratory chemoreception. *Handb Clin Neurol,* 188**,** 37-72.http://dx.doi.org/10.1016/b978-0-323-91534-2.00007-2

GUYENET, P. G., STORNETTA, R. L., SOUZA, G., et al. 2019. The Retrotrapezoid Nucleus: Central Chemoreceptor and Regulator of Breathing Automaticity. *Trends Neurosci,* 42**,** 807-824.http://dx.doi.org/10.1016/j.tins.2019.09.002

HUANG, J., WATERS, K. A. & MACHAALANI, R. 2017. Pituitary adenylate cyclase activating polypeptide (PACAP) and its receptor 1 (PAC1) in the human infant brain and changes in the Sudden Infant Death Syndrome (SIDS). *Neurobiol Dis,* 103**,** 70-77.http://dx.doi.org/10.1016/j.nbd.2017.04.002

IKEDA, K., KAWAKAMI, K., ONIMARU, H., et al. 2017. The respiratory control mechanisms in the brainstem and spinal cord: integrative views of the neuroanatomy and neurophysiology. *J Physiol Sci,* 67**,** 45-62.http://dx.doi.org/10.1007/s12576-016-0475-y

KANG, B. J., CHANG, D. A., MACKAY, D. D., et al. 2007. Central nervous system distribution of the transcription factor Phox2b in the adult rat. *J Comp Neurol,* 503**,** 627-41.http://dx.doi.org/10.1002/cne.21409

KASI, A. S., KUN, S. S., KEENS, T. G., et al. 2018. Adult With PHOX2B Mutation and Late-Onset Congenital Central Hypoventilation Syndrome. *J Clin Sleep Med,* 14**,** 2079-2081.http://dx.doi.org/10.5664/jcsm.7542

KORDOWER, J. H., LE, H. K. & MUFSON, E. J. 1992. Galanin immunoreactivity in the primate central nervous system. *J Comp Neurol,* 319**,** 479-500.http://dx.doi.org/10.1002/cne.903190403

LAVEZZI, A. M., WEESE-MAYER, D. E., YU, M. Y., et al. 2012. Developmental alterations of the respiratory human retrotrapezoid nucleus in sudden unexplained fetal and infant death. *Auton Neurosci,* 170**,** 12-9.http://dx.doi.org/10.1016/j.autneu.2012.06.005

LAZARENKO, R. M., MILNER, T. A., DEPUY, S. D., et al. 2009. Acid sensitivity and ultrastructure of the retrotrapezoid nucleus in Phox2b-EGFP transgenic mice. *J Comp Neurol,* 517**,** 69-86.http://dx.doi.org/10.1002/cne.22136

LEVY, J., DROZ-BARTHOLET, F., ACHOUR, M., et al. 2021. Parafacial neurons in the human brainstem express specific markers for neurons of the retrotrapezoid nucleus. *J Comp Neurol,* 529**,** 3313-3320.http://dx.doi.org/10.1002/cne.25191

LEVY, J., FACCHINETTI, P., JAN, C., et al. 2019. Tridimensional mapping of Phox2b expressing neurons in the brainstem of adult Macaca fascicularis and identification of the retrotrapezoid nucleus. *J Comp Neurol,* 527**,** 2875-2884.http://dx.doi.org/10.1002/cne.24713

MEYLEMANS, A., DEPUYDT, P., DE BAERE, E., et al. 2021. Adult-onset congenital central hypoventilation syndrome due to PHOX2B mutation. *Acta Neurol Belg,* 121**,** 23-35.http://dx.doi.org/10.1007/s13760-020-01363-w

OLIVEIRA, L. M., MOREIRA, T. S., KUO, F. S., et al. 2016. alpha1- and alpha2-adrenergic receptors in the retrotrapezoid nucleus differentially regulate breathing in anesthetized adult rats. *J Neurophysiol,* 116**,** 1036-48.http://dx.doi.org/10.1152/jn.00023.2016

PAXINOS, G., FURLONG, T. & WATSON, C. 2020. *Human brainstem: cytoarchitecture, chemoarchitecture, myeloarchitecture*, Academic Press.

PAXINOS, G., XU-FENG, H., SENGUL, G., & WATSON, C 2012. Organization of brainstem nuclei. In The human nervous system *Elsevier***,** 260-327

ROSIN, D. L., CHANG, D. A. & GUYENET, P. G. 2006. Afferent and efferent connections of the rat retrotrapezoid nucleus. *J Comp Neurol,* 499**,** 64-89.http://dx.doi.org/10.1002/cne.21105

RUDZINSKI, E. & KAPUR, R. P. 2010. PHOX2B immunolocalization of the candidate human retrotrapezoid nucleus. *Pediatr Dev Pathol,* 13**,** 291-9.http://dx.doi.org/10.2350/09-07-0682-OA.1

SHI, Y., STORNETTA, D. S., REKLOW, R. J., et al. 2021. A brainstem peptide system activated at birth protects postnatal breathing. *Nature,* 589**,** 426-430.http://dx.doi.org/10.1038/s41586-020-2991-4

SHI, Y., STORNETTA, R. L., STORNETTA, D. S., et al. 2017. Neuromedin B Expression Defines the Mouse Retrotrapezoid Nucleus. *J Neurosci,* 37**,** 11744-11757.http://dx.doi.org/10.1523/JNEUROSCI.2055-17.2017

SOUZA, G., STORNETTA, R. L., STORNETTA, D. S., et al. 2020. Differential Contribution of the Retrotrapezoid Nucleus and C1 Neurons to Active Expiration and Arousal in Rats. *J Neurosci,* 40**,** 8683-8697.http://dx.doi.org/10.1523/jneurosci.1006-20.2020

STORNETTA, R. L., SPIROVSKI, D., MOREIRA, T. S., et al. 2009. Galanin is a selective marker of the retrotrapezoid nucleus in rats. *J Comp Neurol,* 512**,** 373-83.http://dx.doi.org/10.1002/cne.21897

TAKAKURA, A. C., MOREIRA, T. S., STORNETTA, R. L., et al. 2008. Selective lesion of retrotrapezoid Phox2b-expressing neurons raises the apnoeic threshold in rats. *J Physiol,* 586**,** 2975-91.http://dx.doi.org/10.1113/jphysiol.2008.153163

Statements & Declarations

Funding

This work was supported by Australian Research Council (Grant number DP180101890, NNK), Research Training Program Domestic Fee Offset (RSAI8000, YL) and Research Training Program Domestic Stipend (RSAP1000, YL).

502 **Competing Interests**

503 The authors do not have relevant financial or non-financial interests to disclose.

504 **Author Contributions**

505 This study was designed by YL, CES, RM and NNK. IM trained YL in tissue preparation and
506 immunohistochemistry on FFPE tissues. All authors contributed to the methodology validation and
507 experiment troubleshooting. The tissue preparation, experiments, data collection, data analysis and first
508 manuscript draft were produced by YL. NNK, YL, RM and CES revised and modified manuscript drafts.

509 **Data Availability**

510 The datasets generated during the current study are available from the corresponding author on
511 reasonable request.

512 **Ethics approval**

513 Donor tissue was previously collected by the Sydney Brain Bank under UNSW ethics project no.
514 HC#200026. This research project (Project no. HC#200901) was approved by the Human Research
515 Ethics Advisory Panel of the University of New South Wales.

516 **Consent to participate**

517 Informed consent was obtained from individual participants included in the study prior to tissue
518 donation.

519 **Consent to publish**

520 The authors affirm that human research participants provided informed consent for use of their data for
521 publication.

522

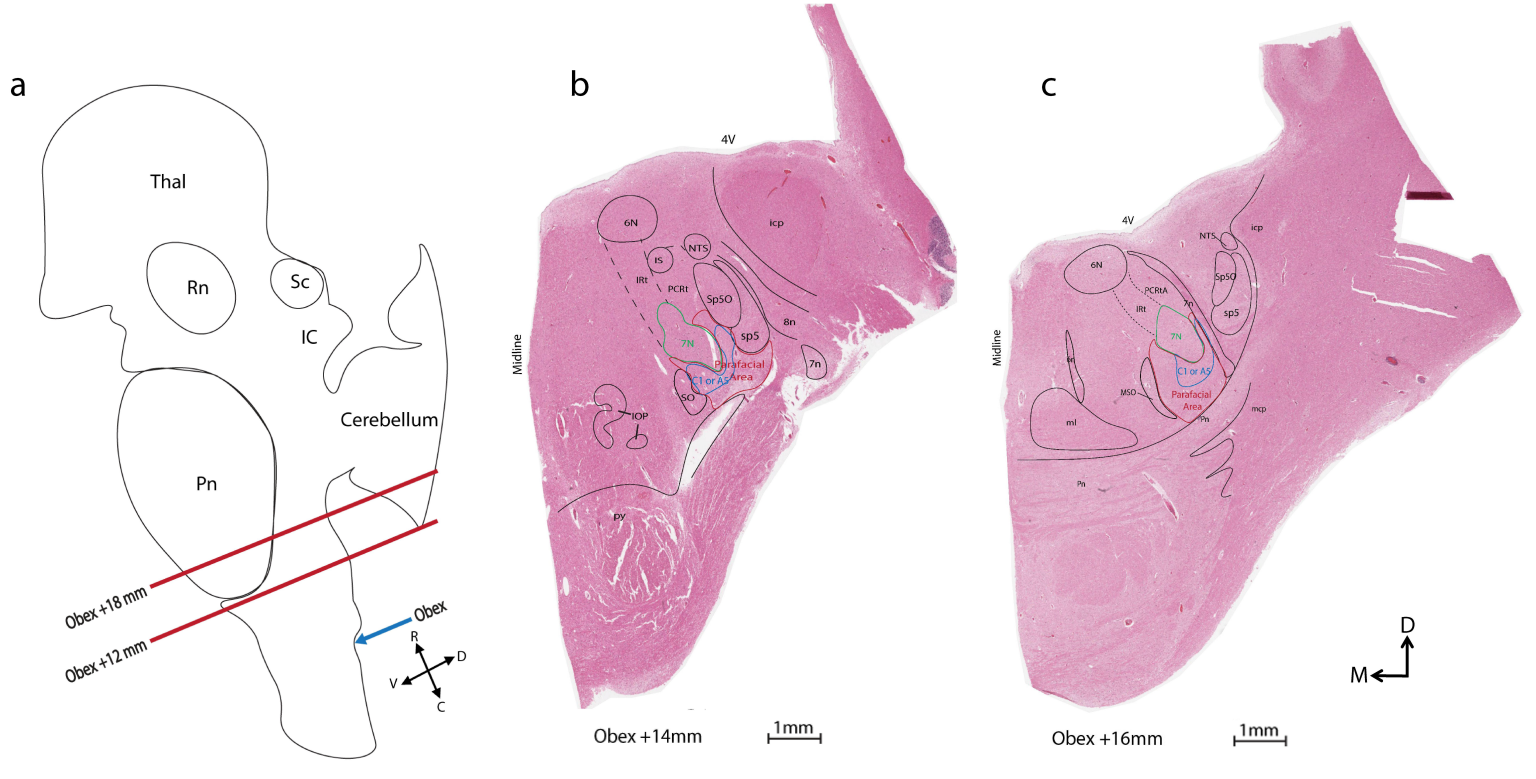
a
Thal
Rn
Sc
IC
Cerebellum
Pn
Obex +18 mm
Obex +12 mm
Obex
R
D
V
C
b
4V
icp
6N
NTS
IS
IRt
PCRt
Sp5O
8n
7N
sp5
Parafacial Area
C1 or A5
7n
SO
IOP
py
Midline
Obex +14mm
1mm
c
4V
NTS
icp
6N
PCRtA
Sp5O
IRt
7n
sp5
7N
6n
C1 or A5
MSO
Parafacial Area
Pn
mcp
ml
Pn
Midline
D
M
Obex +16mm
1mm

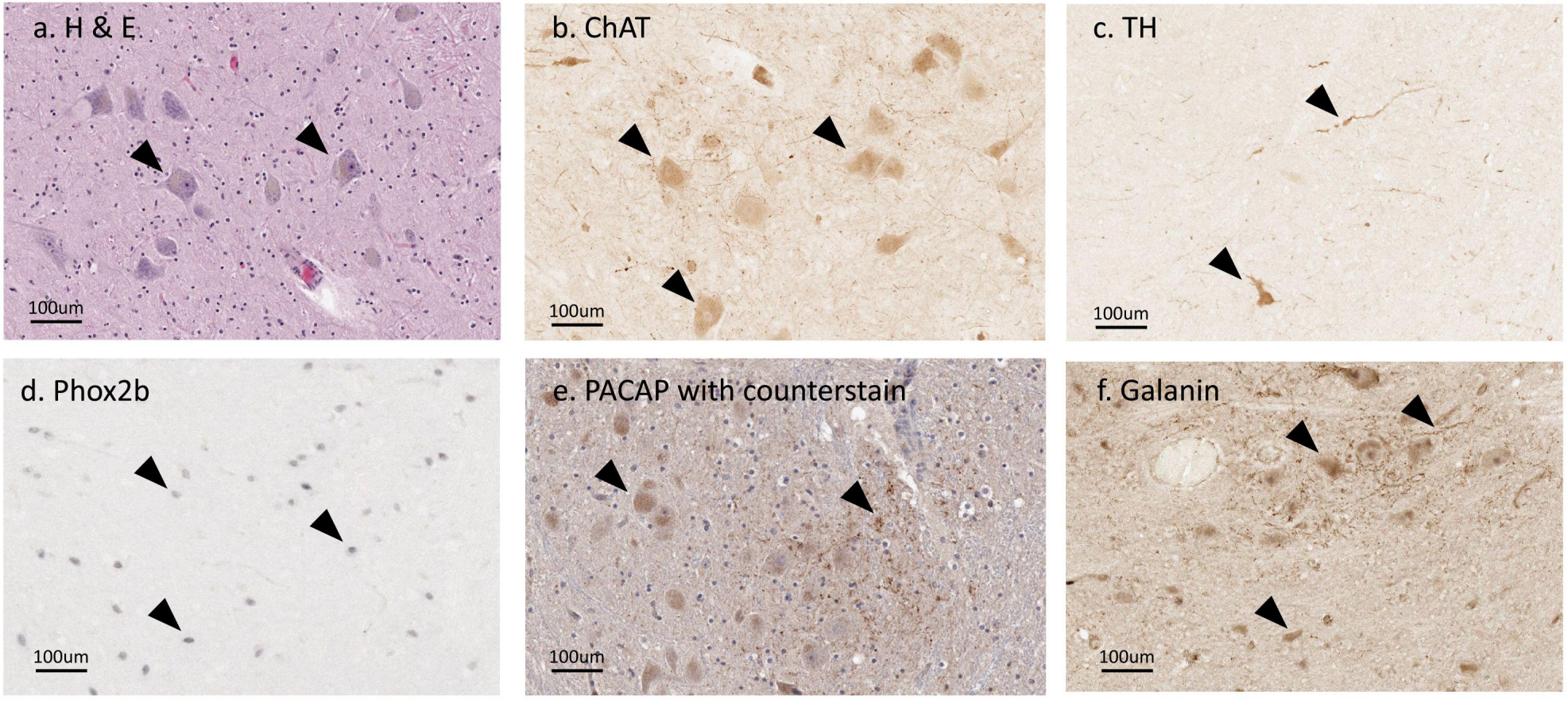
a. H & E
100um
b. ChAT
100um
c. TH
100um
d. Phox2b
100um
e. PACAP with counterstain
100um
f. Galanin
100um

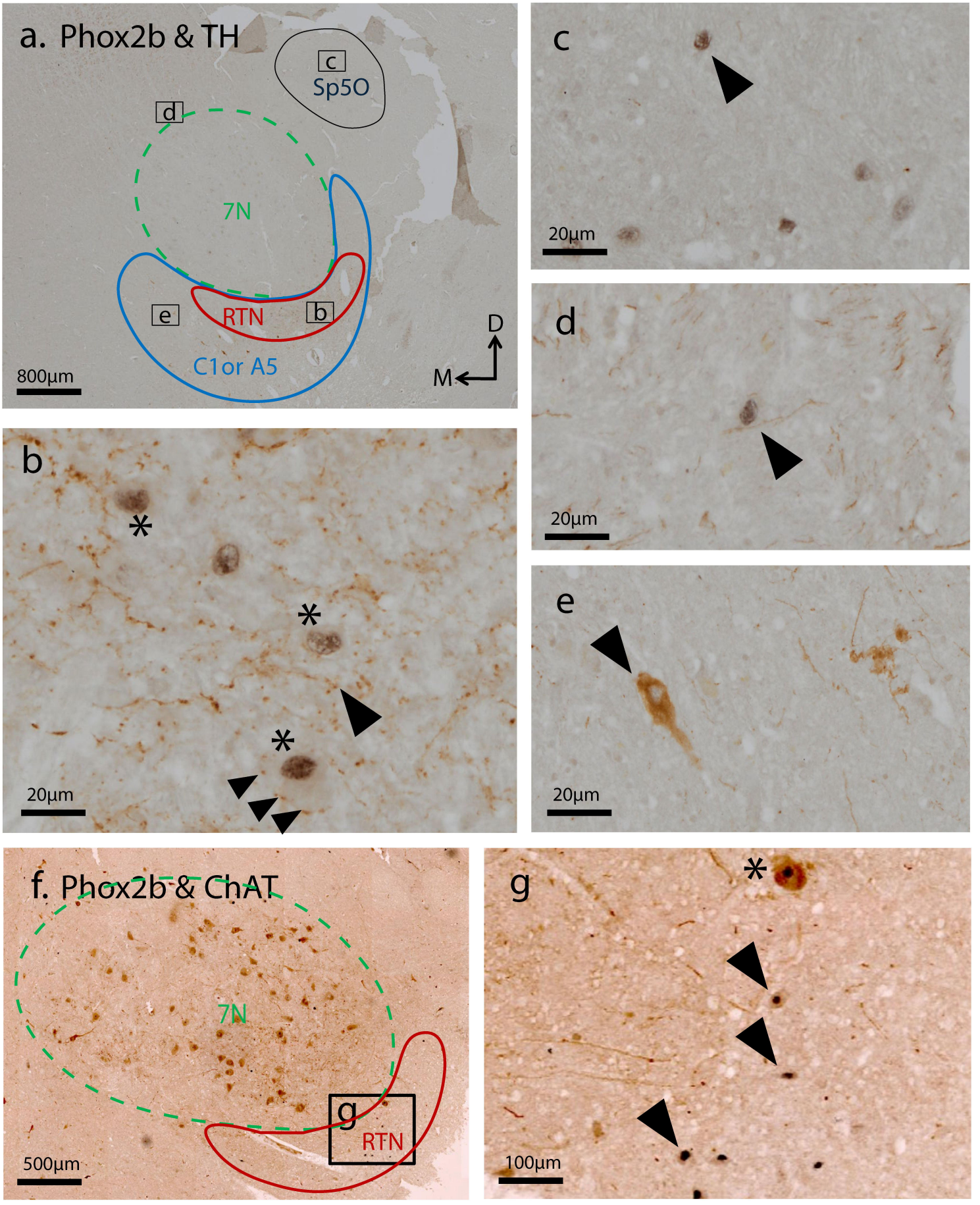
a. Phox2b & TH
c
Sp5O
d
7N
e
RTN
b
C1or A5
D
M
800µm
c
20µm
d
20µm
b
20µm
e
20µm
f. Phox2b & ChAT
7N
g
RTN
500µm
g
100µm

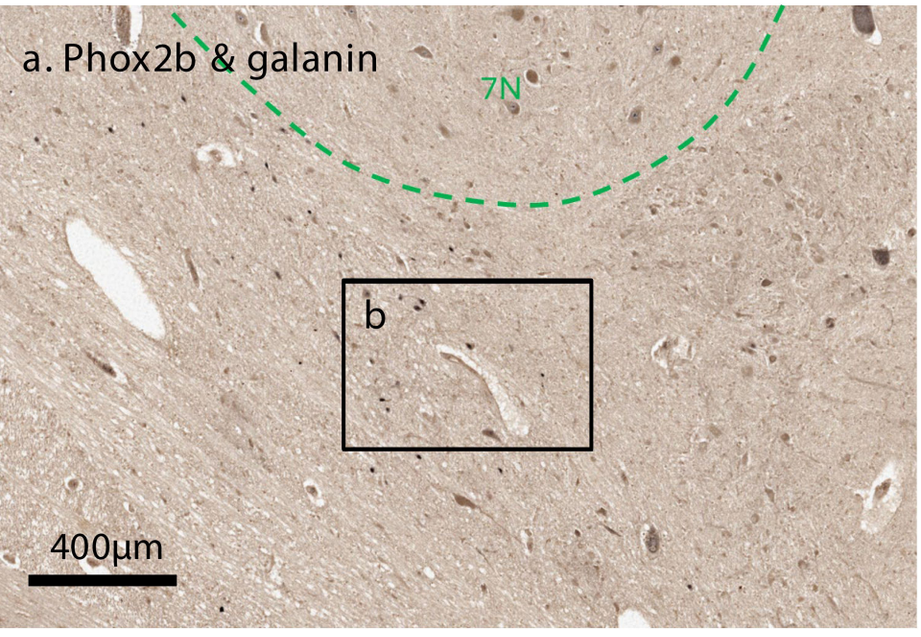
a. Phox2b & galanin
7N
b
400µm

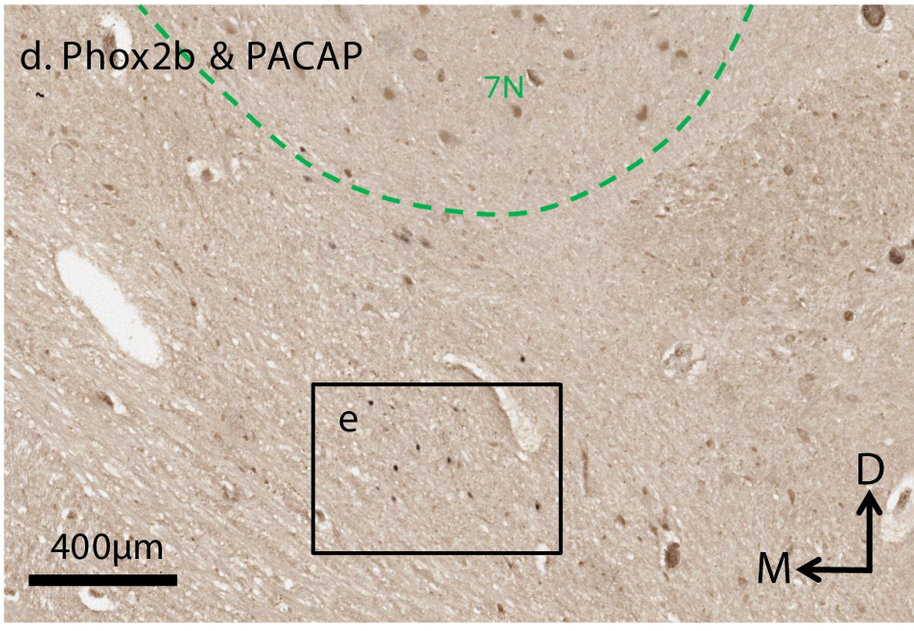
d. Phox2b & PACAP
7N
e
400µm
D
M

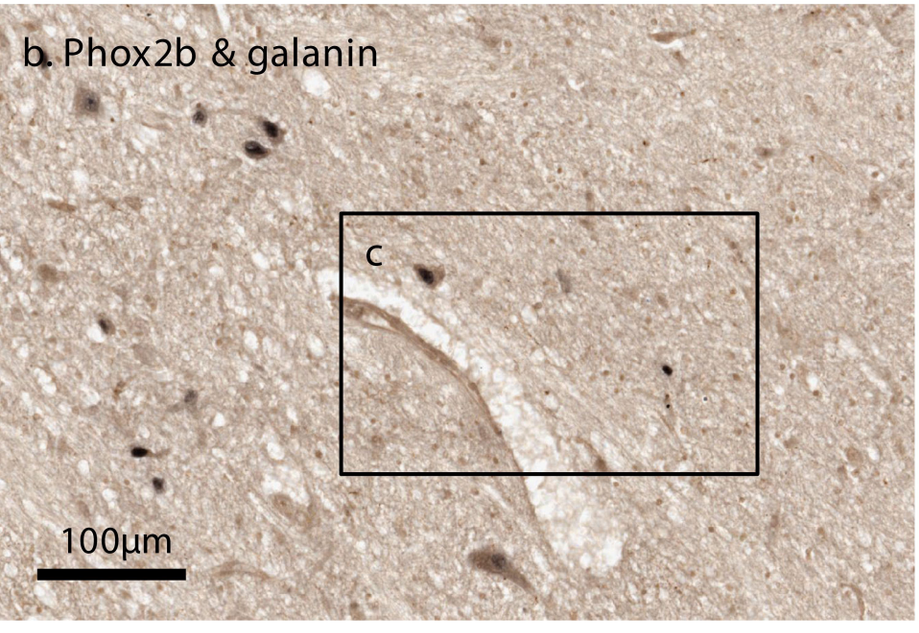
b. Phox2b & galanin
c
100µm

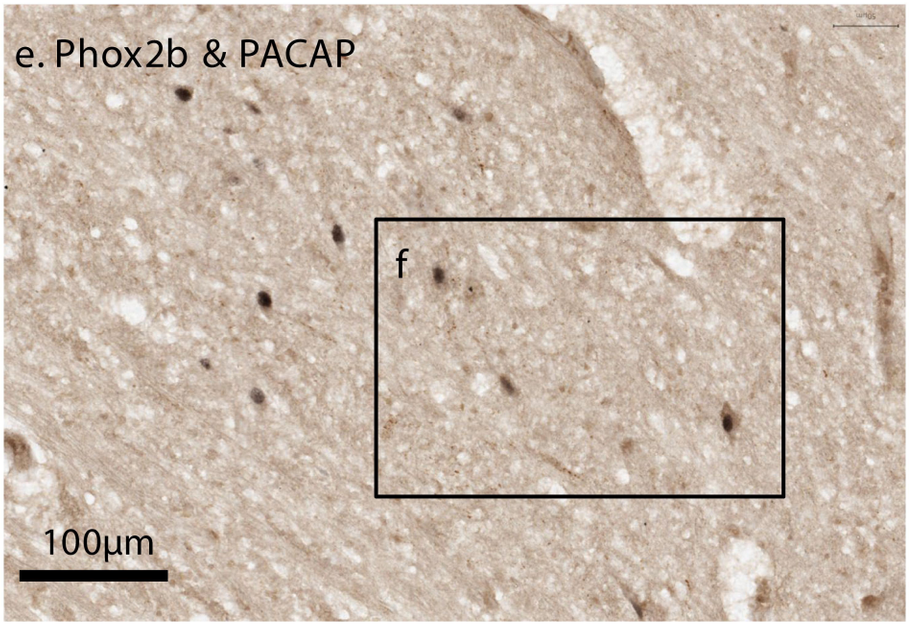
e. Phox2b & PACAP
f
100µm

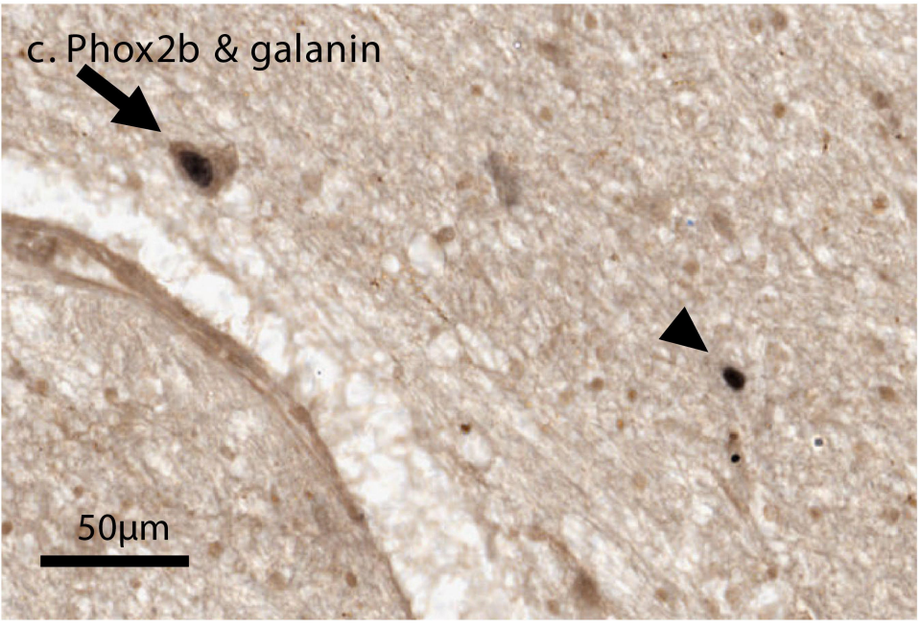
c. Phox2b & galanin
50µm

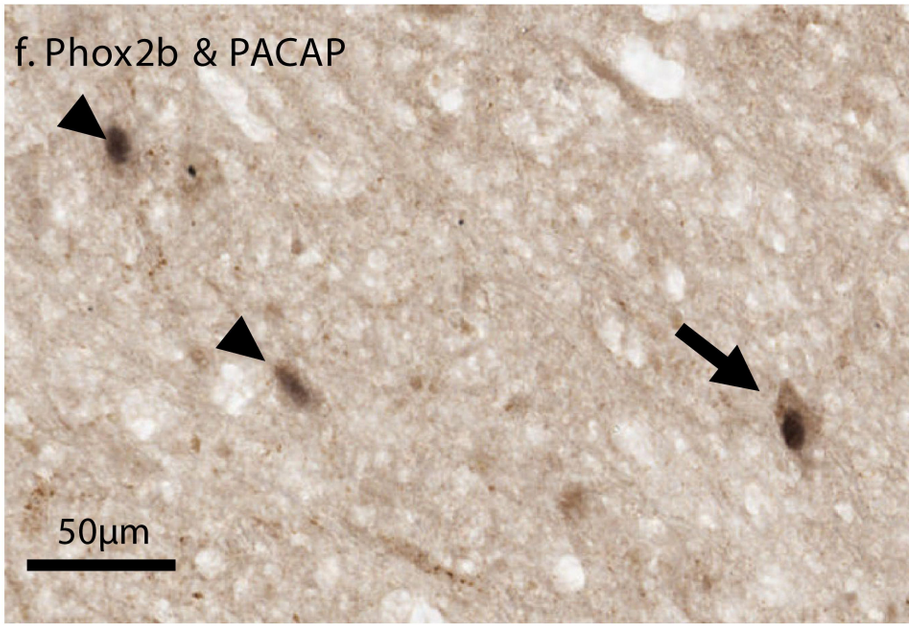
f. Phox2b & PACAP
50µm

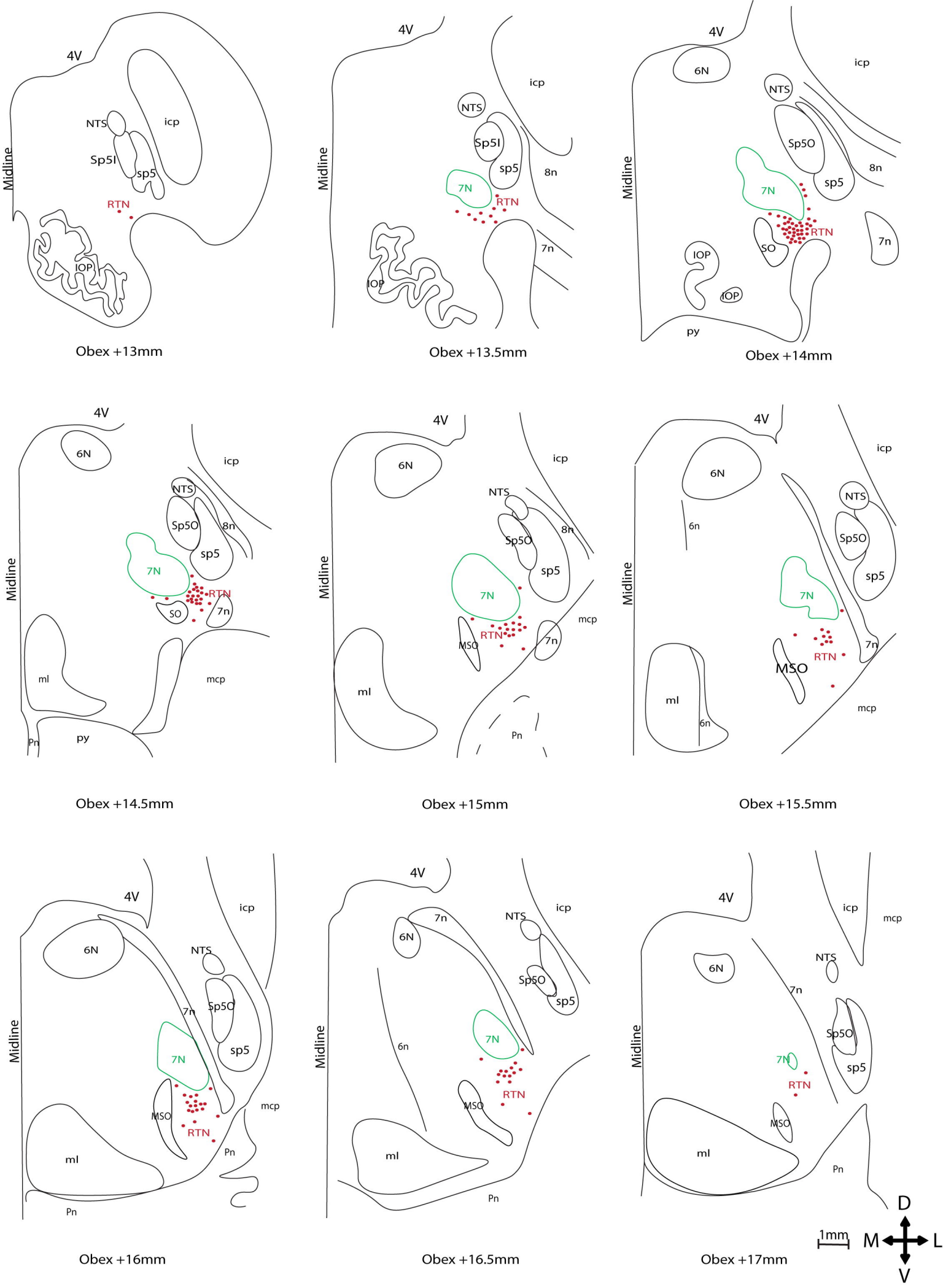
4V
NTS
icp
Sp5I
sp5
RTN
IOP
Midline
Obex +13mm
4V
icp
NTS
Sp5I
sp5
8n
7N
RTN
7n
IOP
Midline
Obex +13.5mm
4V
6N
icp
NTS
Sp5O
8n
sp5
7N
RTN
SO
7n
IOP
IOP
py
Midline
Obex +14mm
4V
6N
icp
NTS
Sp5O
8n
sp5
7N
RTN
SO
7n
ml
mcp
Pn
py
Midline
Obex +14.5mm
4V
6N
icp
NTS
Sp5O
8n
sp5
7N
mcp
RTN
MSO
7n
ml
Pn
Midline
Obex +15mm
4V
icp
6N
NTS
6n
Sp5O
sp5
7N
7n
RTN
MSO
ml
6n
mcp
Midline
Obex +15.5mm
4V
icp
6N
NTS
Sp5O
7n
sp5
7N
mcp
MSO
RTN
ml
Pn
Pn
Midline
Obex +16mm
4V
7n
NTS
icp
6N
Sp5O
sp5
6n
7N
RTN
MSO
ml
Pn
Midline
Obex +16.5mm
4V
icp
mcp
NTS
6N
7n
Sp5O
sp5
7N
RTN
MSO
ml
Pn
Midline
Obex +17mm
1mm
D
M
L
V

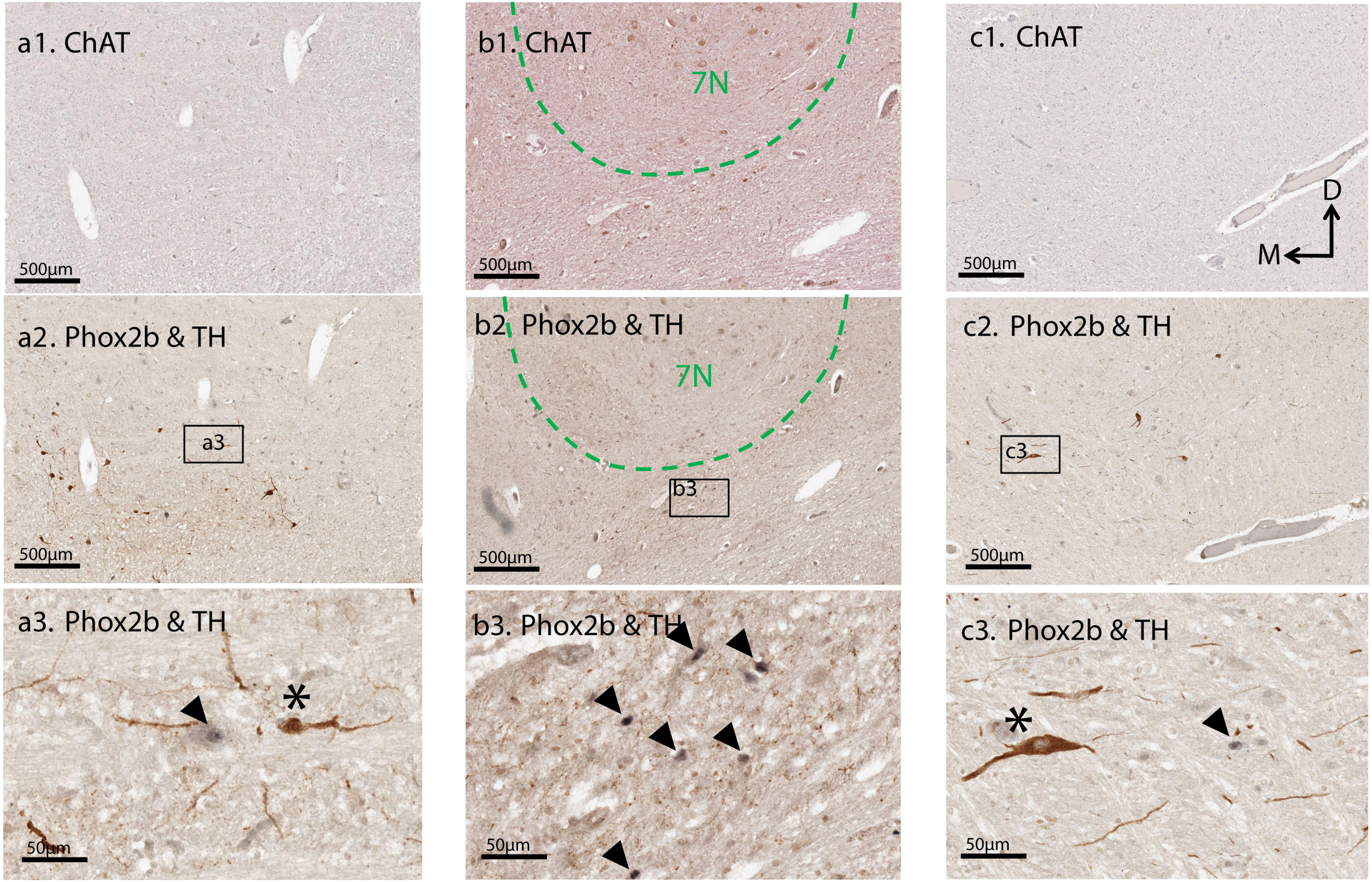

Obex +13.1 mm

Obex +15mm

Obex +16.8 mm

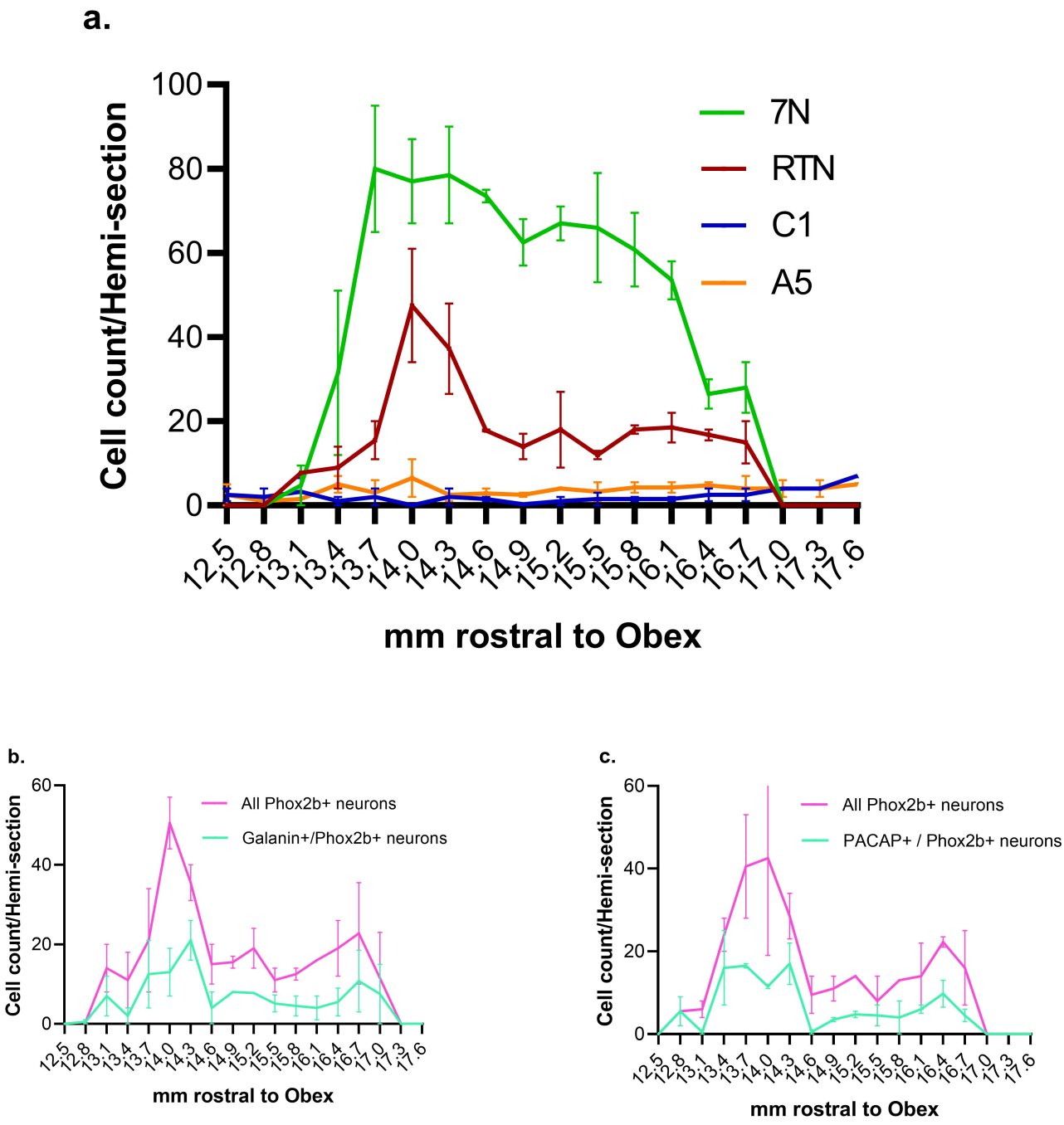
a.
Cell count/Hemi-section
100
80
60
40
20
0
7N
RTN
C1
A5
12.5
12.8
13.1
13.4
13.7
14.0
14.3
14.6
14.9
15.2
15.5
15.8
16.1
16.4
16.7
17.0
17.3
17.6
mm rostral to Obex
b.
Cell count/Hemi-section
60
40
20
0
All Phox2b+ neurons
Galanin+/Phox2b+ neurons
mm rostral to Obex
c.
Cell count/Hemi-section
60
40
20
0
All Phox2b+ neurons
PACAP+ / Phox2b+ neurons
mm rostral to Obex

Developmental age, number of cases, Sex ratio	Tissue Frozen or FFPE, and plane of cut (coronal vs sagittal)	Sections/case analysed; Obex/bregma level	Antibody/probe details & dilution	RTN Phox2b subcellular labelling pattern & anatomical location	Number of RTN neurons (bilateral)	Reference
Human fetuses and infants (19-44w, n=8)	5 µm coronal (n=5) and sagittal (n=3) FFPE sections	1-2 sections/case (level not specified but in the presence of the 7N).	Rabbit anti-Phox2b (gift of J.-F. Brunet, 1:1000). NK1R (Abcam, 1:200); TH (Chemicon, 1:1000)	IHC: cell nucleus. RTN was ventral to 7N and lateral to the SO in the pontomedullary junction.	Not provided	(Rudzinski and Kapur, 2010)
Human fetuses (35-40w, n=9) and infant (2-8 months, n=11)	4 µm coronal FFPE sections	3-6 sections/case: 1-2 sections from each brainstem level of upper pons, upper medulla and from Obex -2/3 mm to +2/3 mm.	Rabbit anti-Phox2b (gift of J.-F. Brunet, 1:750)	IHC: cell nucleus and cytoplasm. RTN located between the 7N and SO in caudal pons.	980 ± 23 Phox2b-ir neurons However, equation applied not provided	(Lavezzi et al., 2012)
Macaca fascicularis (5- & 6-years old males and 16-year-old female, n=2 IHC; n=1 ISH)	40 µm coronal frozen and paraformaldehyde fixed free-floating sections	60 sections/case (1/8 serial sections); Obex -1.40mm to +13mm.	IHC: Rabbit anti-Phox2b antibody (1:2,000; gift from J-F. Brunet) ISH: PPGAL and Phox2b mRNAs	IHC: subcellular location of Phox2b immunoreactivity not described. Parafacial region located ventral and lateral to 7N; ISH: cell cytoplasm. PPGAL+/Phox2b+ RTN neurons located caudal, ventral and lateral to 7N spanning from Obex +4.56 to +10.16 mm.	2400 PPGAL+/ Phox2b+ neurons. PPGAL- /Phox2b neurons were not included. Calculated as an estimation by automated method yet cautions on possibility of double counting.	(Levy et al., 2019)
Human adults (n=2)	10 µm coronal FFPE sections	60 sections/case (1/10 serial sections), Obex +14 mm to +17 mm.	mRNA probes (targeting 237–492 sequence of the galanin message-associated peptide mRNA (i.e. PPGAL) and 469–1173 sequence of the vGlut2 mRNA (SLC17A6) and NMB.	IHC: N/A since Phox2b did not work. ISH: N/A since Phox2b did not work. Based on PPGAL, SLC17A6 and NMB, RTN located in parafacial region.	Not provided	(Levy et al., 2021)
Human adults (n=2)	10 µm coronal FFPE sections	90 sections/case (5/30 serial sections), Obex +12 mm to +18 mm.	Mouse anti-Phox2b (Bio-Strategy Laboratory, cat#sc-376997, 1:1000)	IHC: cell nucleus RTN was identified ventral to 7N, lateral to the SO and medial to facial nerve and Sp5O.	Approximately 5000 Phox2b+TH-ChAT- RTN neurons.	Study herein

Antibody	Source (Catalogue Number), RRID	Immunogen	Validation	Target & expected subcellular labelling	Dilution
Primary (1°) Antibodies					
Mouse monoclonal anti-Phox2b IgG antibody	Bio-Strategy Laboratory (sc-376997), RRID: AB_2813765	Human origin N-term amino acids 11-70	IHC: cross-reactivity with mouse brain tissue ISH: co-localisation with Phox2b mRNA labelled using RNAscope (Dereli et al., 2021)	Phox2b transcription factor (e.g. nucleus of RTN and C1 neurons)	1:1000
Chicken anti-Tyrosine Hydroxylase (TH)	Aves Labs (TYH-0020), RRID: AB_10013440	Human tyrosine hydroxylase (E.C.1.14.16.2) protein	IF: human gastric tissue (Eicher et al., 2022).	Catecholaminergic neurons (e.g. cytoplasm of C1 neurons)	1:6000
Goat anti-Choline Acetyltransferase (ChAT)	Millipore Sigma (AB144P), RRID: RRID AB_2079751	Human placental enzyme	IHC: rat brain tissue (1:200) (Bhagwandin et al., 2006); IHC: ape brain tissue (1:3000) (Williams et al., 2022)	Cholinergic neurons (e.g. cytoplasm of 7N)	1:1000
Rabbit anti-Galanin	Peninsula Laboratories International (T-4325), RRID: not provided	Synthetic peptide H-Gly-Trp-Thr-Leu-Asn-Ser-Ala-Gly-Tyr-Leu-Leu-GlyPro-His-Ala-Val-Gly-Asn-His-Arg-Ser-Phe-Ser-Asp-Lys-Asn-Gly-LeuThr-Ser-OH coupled to carrier protein.	IHC: human brain tissue (1:300)(Falkenstetter et al., 2020)	Galaninergic neurons (e.g. cytoplasm of NTS and RTN neurons)	1:300
Rabbit anti-PACAP	Abcam (ab216627), RRID: Not provided	Human ADCYAP1 aa 150 to C-terminus	IF: Pig nerve fibers in the aortic arch wall (1:4000) (Rytel et al., 2022); IHC: mouse brain tissue (1:700) (Hu et al., 2020).	PACAP neuropeptide (e.g. cytoplasm of NTS and RTN neurons)	1:300
Secondary (2°) Antibodies					
Biotin-SP-conjugated Donkey anti-Mouse IgG	Jackson ImmunoResearch (715-035-150), RRID: AB_2340770	Whole molecule mouse IgG	WB: Human HeLa cells (1:10000) (Srinivasan et al., 2024)	Mouse anti-Phox2b 1° Ab	1:500
Biotin-SP-conjugated Donkey anti-Chicken IgG	Jackson ImmunoResearch (703-065-155), RRID: AB_2313595	Whole molecule chicken IgY	IHC: mouse eyes (dilution not provided) (Little et al., 2020)	Chicken anti-TH 1° Ab	1:500
Biotin-SP-conjugated Donkey anti-Goat IgG	Jackson ImmunoResearch (705-065-147), RRID: AB_2340397	Whole molecule goat IgY	IHC: Mouse brain and spine tissue (1:500) (Agostinelli et al., 2021)	Goat anti-ChAT 1° Ab	1:500
Biotin-SP-conjugated Donkey anti-Rabbit IgG	Jackson ImmunoResearch (711-065-152), RRID: AB_2340593	Whole molecule rabbit IgY	WB: Human HeLa cells (1:10000) (Srinivasan et al., 2024)	Rabbit anti-PACAP 1° Ab	1:500

Cell Type	Morphology	Nucleus: Area (μm^2)	Cell Area (μm^2)	Cell Diameter (μm)	Subcellular neurochemical profile		
					Cytoplasm	Nucleus	Axon
7N neurons (n=68, 1 section/case)	Large multipolar neurons with short dendrites	274.6 ± 108	1194.0 ± 371.8	41.8 ± 10.7	ChAT+, TH-, PACAP+/-, galanin-	Phox2b+/-	ChAT+
RTN neurons (n=241, 3 sections/case)	Medium round or fusiform neurons with short dendrites	69.0 ± 23.3	309.9 ± 61.8	19.9 ±4.0	ChAT-, TH-, PACAP+/-, Galanin+/-	Phox2b+	Not detected
C1 neurons (n=38, 4 sections/case)	Medium multipolar neuron with short dendrites and long projecting axons	98.0 ± 51.2	528.2 ± 165.2	35.1±8.9	ChAT-, TH+, PACAP+/-, galanin-	Phox2b+	TH+
A5 neurons (n=12, 4 sections/case)	Medium multipolar neuron with short dendrites and long projecting axons	101.3 ± 44.9	468.7 ± 169.4	33.9 ±11.7	ChAT-, TH+, PACAP+/-, galanin-	Phox2b-	TH+

Mean ± standard deviation.

	Phox2b+ RTN neurons *	Phox2b+ parafacial neurons	Phox2b+/ PACAP+ parafacial neurons	Phox2b+/galanin+ parafacial neurons	% of Phox2b+ parafacial PACAP+ neurons	% of Phox2b+ parafacial galanin+ neurons
Case 1	5300	5960	2420	2985	41	50
Case 2	4903	4630	1760	1540	38	33
Average	5102	5295	2090	2262	39	43

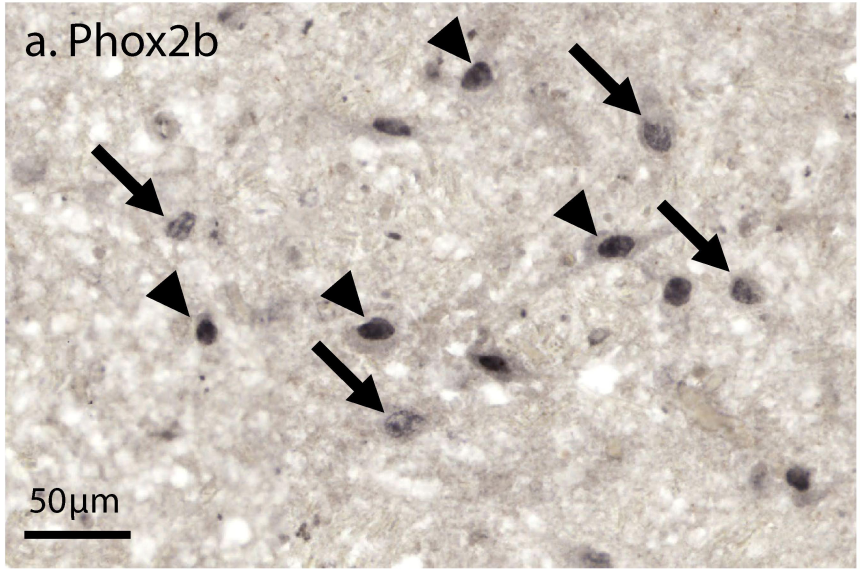
a. Phox2b
50µm

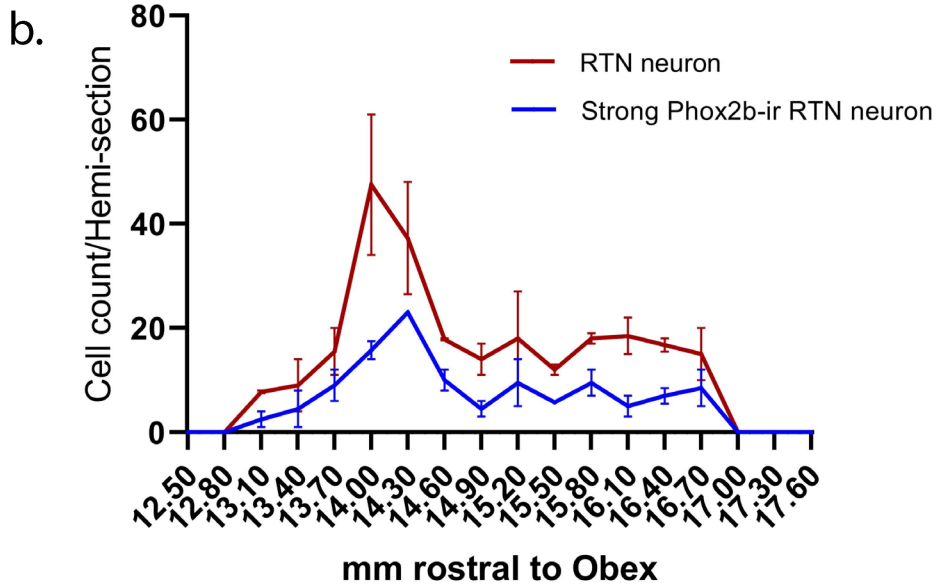
b.
RTN neuron
Strong Phox2b-ir RTN neuron
Cell count/Hemi-section
0
20
40
60
80
12.50
12.80
13.10
13.40
13.70
14.00
14.30
14.60
14.90
15.20
15.50
15.80
16.10
16.40
16.70
17.00
17.30
17.60
mm rostral to Obex

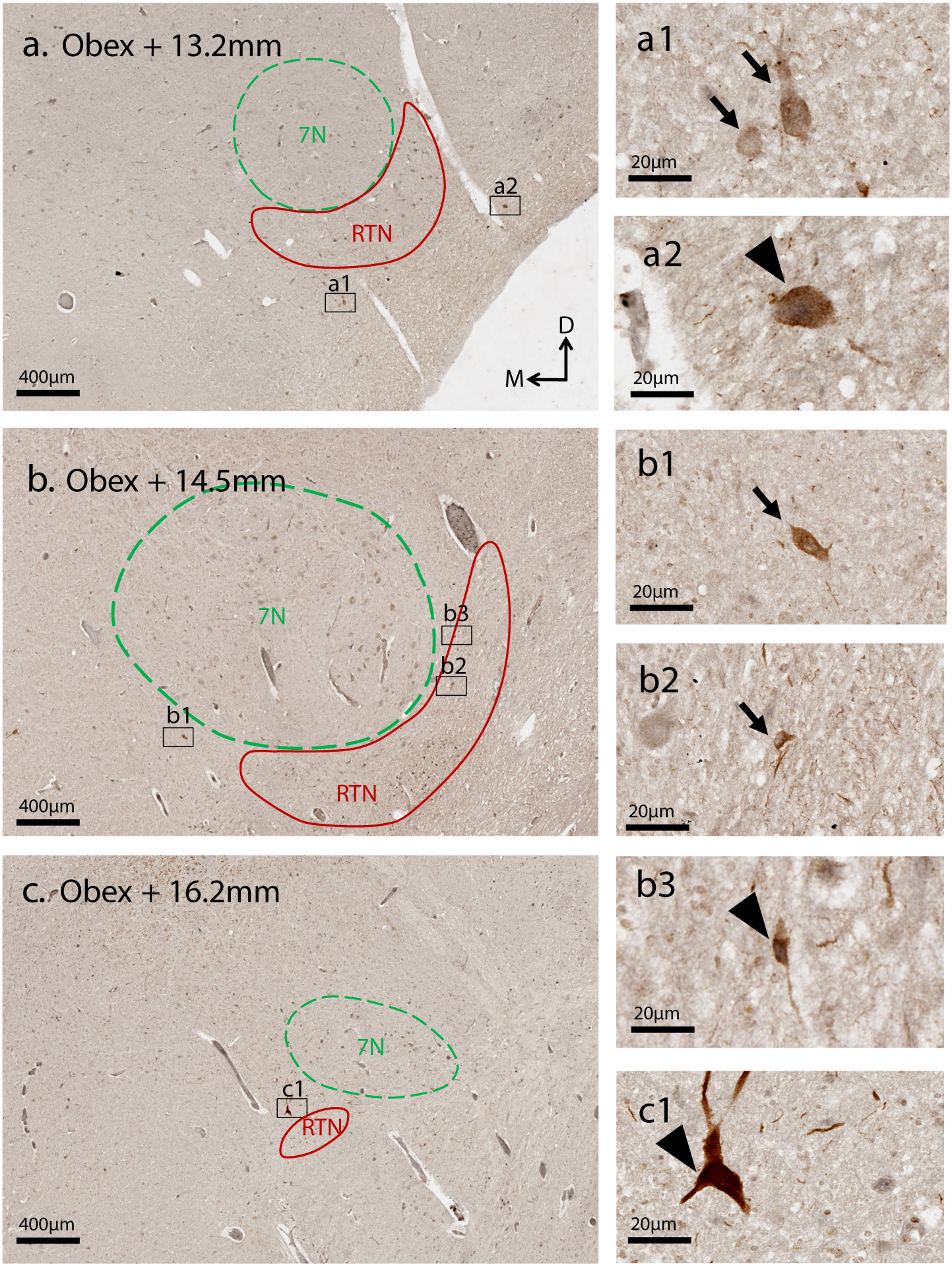
a. Obex + 13.2mm
7N
RTN
a1
a2
D
M
400µm
a1
20µm
a2
20µm
b. Obex + 14.5mm
7N
b1
b2
b3
RTN
400µm
b1
20µm
b2
20µm
c. Obex + 16.2mm
7N
c1
RTN
400µm
b3
20µm
c1
20µm